miR-16 targets Bcl-2 in paclitaxel-resistant lung cancer cells and overexpression of miR-16 along with miR-17 causes unprecedented sensitivity by simultaneously modulating autophagy and apoptosis

Abhisek Chatterjee, Dhrubajyoti Chattopadhyay, Gopal Chakrabarti *

Department of Biotechnology and Dr. B.C. Guha Centre for Genetic Engineering and Biotechnology, University of Calcutta, 35 Ballygunge Circular Road, Kolkata, WB 700019, India

A B S T R A C T

Non-small cell lung cancer is one of the most aggressive cancers as per as the mortality and occurrence is concerned. Paclitaxel based chemotherapeutic regimes are now used as an important option for the treatment of lung cancer. However, resistance of lung cancer cells to paclitaxel continues to be a major clinical problem nowadays. Despite impressive initial clinical response, most of the patients eventually develop some degree of paclitaxel resistance in the course of treatment. Previously, utilizing miRNA arrays we reported that downregulation of miR-17 is at least partly involved in the development of paclitaxel resistance in lung cancer cells by modulating Beclin-1 expression [1]. In this study, we showed that miR-16 was also significantly downregulated in paclitaxel resistant lung cancer cells. We demonstrated that anti-apoptotic protein Bcl-2 was directly targeted miR-16 in paclitaxel resistant lung cancer cells. Moreover, in this report we showed that the combined overexpression of miR-16 and miR-17 and subsequent paclitaxel treatment greatly sensitized paclitaxel resistant lung cancer cells to paclitaxel by inducing apoptosis via caspase-3 mediated pathway. Combined overexpression of miR-16 and miR-17 greatly reduced Beclin-1 and Bcl-2 expressions respectively. Our results indicated that though miR-17 and miR-16 had no common target, both miR-16 and miR-17 jointly played roles in the development of paclitaxel resistance in lung cancer. miR-17 overexpression reduced cytoprotective autophagy by targeting Beclin-1, whereas overexpression of miR-16 potentiated paclitaxel induced apoptotic cell death by inhibiting anti-apoptotic protein Bcl-2.

© 2014 Published by Elsevier Inc.

1. Introduction

Worldwide, lung cancer appears to be one of the most commonly diagnosed cancers causing almost 1.38 million deaths and 1.61 million new occurrences each year [2]. Taxens, specially paclitaxel has emerged as an important, broad range chemotherapeutic agent since paclitaxel based combination chemotherapies are now being globally prescribed as standard therapies in the treatment of lung cancer as well as other cancers such as breast, ovarian, and prostate [3–5]. However, despite its wide spread usage, resistance of cancer cells to paclitaxel has become frequent and has been recognized as the major reason for reoccurrence, cancer progression and failure of therapy in many cancer types [6].

During paclitaxel resistance, the cancer cells eventually escape the paclitaxel induced apoptotic death and this failure of paclitaxel treatment to induce apoptosis ultimately contributes to relapse and poor prognosis [1,3,4,7–9]. In the last couple of years considerable amount of research is going on to understand the mechanism of paclitaxel resistance to overcome the problem of drug resistance in paclitaxel therapy.

MicroRNAs (miRNAs) are endogenous non-protein coding, single stranded RNA of ~22 nucleotide length which plays important roles in controlling gene expression in humans [10]. miRNAs guide the RNA-induced silencing complex (RISC) to bind to the complementary sequences within the 3′ untranslated region of the cognate mRNA and thereby either translationally repress the mRNA expression or induce destabilization and degradation of the target mRNA bearing fully complementary target sites [10,11]. Previous studies involving NCI-60 panel of cell lines have shown that miRNA expression patterns are better representative of the type and stage in human cancers than classical mRNA profiles [12]. Moreover, dysregulated miRNA expression has already been reported in the case of various human malignancies including non-small cell lung cancer (NSCLC) [1,3,13].

We have been working on the role of miRNA in the development of paclitaxel-resistance in lung cancer cells. In our previous report, we

performed miRNA array analysis to screen differentially expressed miRNAs between paclitaxel resistant and paclitaxel sensitive lung cancer cells and we reported that downregulation of miR-17 contributed to the development of paclitaxel resistance of lung cancer cells by increasing Beclin-1 expression and subsequent autophagy [1]. From the microarray data we found that miR-16 was also significantly downregulated in paclitaxel resistant lung cancer cells. So in this current study, we first investigated the role of downregulation of miR-16 in the development of paclitaxel-resistance in lung cancer cells and then we determined the effect of combined overexpression of miR-16 and miR-17 and subsequent paclitaxel treatment in modulating the sensitivity of resistant cells to paclitaxel. We demonstrated that anti-apoptotic protein Bcl-2 was a direct target of miR-16 in paclitaxel resistant lung cancer cells. Ectopic expression of miR-16 into paclitaxel resistant lung cancer cells significantly sensitized the cells to paclitaxel.

Since it is understood that downregulation of a single miRNA cannot be held solely responsible for the development of paclitaxel resistance. Other miRNAs could be involved in this process. We previously found that miR-17 was involved in the development of paclitaxel resistance in lung cancer cells [1]. So we were interested to compare the effects of combined overexpression of miR-16 and miR-17 and subsequent paclitaxel treatment with the effects of individual miRNA overexpression (miR-16 or miR-17 individually) more clearly, we showed the results for individual miR-16 or miR-17 overexpression and subsequent paclitaxel treatment in parallel with the combined miR-16 and miR-17 overexpression results. Our data clearly demonstrated that both miR-16 and miR-17, without having a common target, jointly played role in the development of paclitaxel resistance in lung cancer cells and combined inhibition of Beclin-1 mediated autophagy by miR-17 overexpression and downregulation of anti-apoptotic protein Bcl-2 by miR-16 overexpression stimulated ROS generation, which was required for paclitaxel mediated apoptotic cell death in paclitaxel resistant lung cancer cells.

2. Materials and methods

2.1. Reagents and antibodies

Nutrient mixture Dulbecco's Modified Eagle's Medium (supplemented with 1 mM L-glutamine), FBS (fetal bovine serum), penicillin–streptomycin, amphotericin B and 0.25% Trypsin–EDTA were purchased from GIBCO (Invitrogen, USA). Annexin V–FITC apoptosis detection kit was obtained from BD Bioscience, USA. Paclitaxel (Tx), JC-1, H2-DCFDA, zVAD-fmk, MTT, monodansylcadaverine (MDC), acridine orange (A.O) and anti-Bax antibody (mouse monoclonal) were purchased from Sigma, USA. The antibodies to anti-PI3K (p85) (rabbit monoclonal), anti-cleaved caspase 9 (Asp330, rabbit monoclonal), anti-cleaved PARP (Asp214, human specific, mouse monoclonal) (89 kDa), anti-Akt (mouse monoclonal), anti-phospho-Akt (mouse monoclonal) and anti-GAPDH (mouse monoclonal) were obtained from Cell Signaling Technology (Beverly, MA, USA). Anti-cleaved caspase 3 (Asp175, rabbit monoclonal) was from Merck Millipore, Germany. Anti-phospho-tyrosin (PY20) (mouse monoclonal) and anti-mTOR antibody (N-19, goat polyclonal) were obtained from Santa Cruz Biotechnology, USA. Bradford protein estimation kit was purchased from Genei, India. All other chemicals and reagents were of analytical grade and were purchased from Sisco Research Laboratories, India.

2.2. Cell line and cell culture

Human non-small lung epithelial adenocarcinoma cell line Type II, A549, was obtained from the cell repository of the National Centre for Cell Science (NCCS), Pune, India. Human lung adenosquamous carcinoma cell line NCI-H596 and human non-small cell lung adenocarcinoma cell lines NCI-H1734 and NCI-H1299 were obtained from American Type Culture Collection (ATCC). All the cell lines were characterized

by mt-rDNA sequencing for species identification, short tandem repeat profiling and isoenzyme analysis for cell line authentication and were confirmed not to be mycoplasma contaminated by the repository. Cells were selected for resistance to paclitaxel in a stepwise manner essentially as described in [1]. All the cell lines were cultured in Dulbecco's Modified Eagle's Medium (DMEM) supplemented with 1 mM L-glutamine, 10% FBS, 3.7 g/l NaHCO$_3$, 100 μg/ml each of penicillin and streptomycin and 2.5 μg/ml amphotericin B. Cells were maintained at 37 °C in a humidified atmosphere containing 5% CO$_2$. Cells were grown up to ~80% confluency in tissue culture plates, then trypsinized with 0.25% Trypsin–EDTA and divided into subsequent culture plates as required.

2.3. Pre-miRNA transfection

mirVana miRNA 17 mimic precursor (pre-miR-17), mirVana miRNA 16 mimic precursor (pre-miR-16) and mirVana miRNA mimic negative control #1 (pre-miR-negative control) were purchased from Ambion, USA. Pre-miRNAs were transfected into cell lines at ~50% confluency at 100 nM concentration with Lipofectamine RNAiMAX (Invitrogen) transfection reagent. Forty-eight hours after transfection, the expressions of miRNAs were detected by real-time PCR and the expressions of Beclin-1 and Bcl-2 were analysed by qRT-PCR and/or Western blotting.

2.4. Quantitative real-time PCR (qRT-PCR)

TaqMan qRT-PCR was performed to evaluate the expression of miRNAs using the TaqMan microRNA reverse transcription kit (Applied Biosystems, USA) and TaqMan microRNA assays kit (Applied Biosystems, USA) following the manufacturer's protocols. Expression of U6 SnRNA was used as the internal reference to normalize the relative miRNA expression data. To analyze the expression of Bax, Beclin-1, Bcl-2, p62, LC3-II and glyceraldehyde-3-phosphate dehydrogenase (GAPDH) (Table 1) cDNAs were prepared from 2 μg of total RNA using SuperScript VILO cDNA Synthesis kit (Invitrogen, USA). Requisite amount of cDNA was mixed with 2× DyNAmo ColorFlash SYBR Green qPCR Master Mix (Thermo Scientific) and various sets of gene-specific primers (Table 1) and then subjected to qRT-PCR quantification using the StepOne-Plus real time PCR system (Applied Biosystems, USA). Gene expression was normalized with respect to GAPDH (for Beclin-1, Bax, Bcl-2, LC3-II, p62 etc.) or U6 SnRNA (for miR-17 and miR-16) using the comparative cycle time (Ct) method ($2^{-\Delta\Delta Ct}$ method) [14].

2.5. Cell proliferation inhibition assay (MTT assay)

A549-T24 and H596-TxR cells, either transfected with 100 nM pre-miR-17 (T24-miR-17 and TxR-miR-17 respectively) or with 100 nM pre-miR-16 (T24-miR-16 and TxR-miR-16) or with 50 nM each of both pre-miR-17 and pre-miR-16 (T24-miR-comb and TxR-miR-comb) or with 100 nM pre-miR-negative control RNA (T24-miR-NC and TxR-miR-NC respectively) were plated in 96-well culture plates (1

Table 1
Primer sequences used for real-time PCR.

Gene name	Forward primer sequence (5′–3′)	Reverse primer sequence (5′–3′)
Bcl-2	TTGGATCAGGGAGTTGGAAG	TGTCCCTACCAACCAGAAGG
LC3-II	GAGAAGCAGCTTCCTGTTCTGG	GTGTCCGTTCACCAACAGGAAG
Beclin-1	CAAGATCCTGGACCGTGTCA	TGGCACTTTCTGTGGACATCA
p62	TGTGGAACATGGAGGGAAGAG	TGTGCCTGTGCTGGAACTTTC
Bax	GGACGAACTGGACAGTAACATGG	GCAAAGTAGAAAAGGGCGACAAC
P53	GTTCCGAGAGCTGAATGAGG	TTATGGCGGGAGGTAGACTG
GAPDH	CACCATGGAGAAGGCTGGGGCTC	GCCCAGGATGCCCTTGAGGG

× 10^4 cells per well). After 24 h incubation cells were treated with different concentrations (0–200 nM) of paclitaxel for another 48 h. MTT (5 mg/ml) was dissolved in PBS and filter sterilized. Then 20 μl of the prepared solution was added to each well. This was incubated until purple precipitate was visible. Subsequently, 100 μl of Triton X-100 was added to each well and incubated in darkness for 2 h at room temperature. The absorbance was measured on a microplate reader (VersaMax Absorbance Microplate Reader, Molecular Devices, California, USA) at a test wavelength of 570 nm and a reference wavelength of 650 nm. Data were calculated as the percentage of inhibition by the following formula:

$$\%\text{inhibition} = [100 - (A_t/A_s) \times 100] \times \%. \tag{1}$$

A_t and A_s indicated the absorbance of the test substances and solvent control, respectively [1].

2.6. Trypan blue exclusion assay for cell viability

Trypan blue exclusion assay [15] was used to determine the number of viable and dead cells following pre-miR-16 transfection and subsequent paclitaxel treatment. Briefly, T24-miR-16 or T24-miR-NC cells were plated in 6-well culture plates (5×10^4 cells per well). Then cells were treated with 24 nM paclitaxel for another 48 h. After 48 h cells were harvested through trypsinization, washed twice with $1\times$ PBS and then stained with 0.4% trypan blue in PBS. Cells were then prepared for analysis by flow cytometry.

2.7. Adherent colony formation assay

T24-miR-NC, T24-miR-17, T24-miR-16 and T24-miR-comb cells were seeded in triplicate in 6 well plates at a density of 1000 cells per well. The cells were allowed to attach to the substratum for 24 h and subsequently treated with 12 nM paclitaxel for 48 h. The cells were then washed twice with sterile PBS and fresh culture media was added to each well. The cells were allowed to grow for 15 days at 37 °C, 5% CO_2 with media changes in every 3–4 days until colonies were visible by the eye. The media were aspirated and the colonies were fixed with 4% paraformaldehyde solution at room temperature and stained with 0.5% crystal violet solution. Excess stain was washed out and the plates were air dried. The stained colonies were photographed using Bio-rad ChemiDoc XRS + molecular imager. Colony formation was quantitated by dissolving stained cells in Sorenson's buffer (0.1 mol/l sodium citrate, 50% ethanol, pH 4.2) for colorimetric reading of absorbance at 550 nm [16].

2.8. Immunoprecipitation

A549 and A549-T24 cells (1×10^8 cells/ml) were washed twice with PBS and incubated on ice for 30 min with 1 ml lysis buffer [50 mM Tris–HCl, pH 7.5, 100 mM NaCl, 2 mM EDTA, 1% CHAPS (w/v), 50 mM NaF, 200 nM okadaic acid, 1 mM Na_3VO_4, and protease inhibitor cocktail (complete Mini; Roche Applied Science)]. Cell lysates were centrifuged at 20,000 ×g for 15 min at 4 °C. Protein concentrations of the cell lysates were measured by Bradford's method using BSA as standard [17]. Equal amounts of the resulting supernatants (400 μl) were incubated with antibody against Bcl-2 (2 μg/IP tubes) overnight at 4 °C. Moreover, for PI3K co-immunoprecipitation experiments, cells (3×10^6 cells/ml) were either transfected with pre-miR-negative control RNA (T24-miR-NC) or with pre-miR-17 (T24-miR-17) or with pre-miR-16 (T24-miR-16) or with both pre-miR-17 and pre-miR-16 (T24-miR-comb) and subsequently treated with 12 nM paclitaxel for 48 h. Cells were washed twice with PBS and extracted in 1 ml cold lysis buffer (composition mentioned earlier). The cell lysates were centrifuged and the supernatants (400 μl) were incubated with antibody against the p85 (2 μg/IP tubes)

regulatory subunit of PI3K overnight at 4 °C. 50 μl protein A/G agarose beads (Pierce, Thermo Scientific) were added to each IP tube (for both p85 and Bcl-2 IP) and were incubated for 4 h at 4 °C under shaking condition. Nonspecific control antibody used was rabbit serum IgG (1:200 dilution; Life Technologies, USA). The beads were washed four times with lysis buffer and boiled for 5 min in 50 μl 1× sample buffer. The eluted proteins were resolved by 12% SDS-PAGE and analyzed by immuno-blotting. Proteins were transferred to nitrocellulose membranes (Thermo Scientific, USA) and immunoblotted either for p85 and p-Tyr (PY20) to determine total and phosphorylated p85 or for Bcl-2, Beclin-1 and inositol 1,4,5-trisphosphate receptor.

2.9. Immunoblotting

Cells were lysed in lysis buffer containing 50 mM Tris pH 7.5, 150 mM NaCl, 1% Triton X-100, 0.1% (w/v) sodium dodecyl sulphate, 200 mM DTT and a cocktail of protease inhibitors (complete Mini; Roche Applied Science) for 30 min at 4 °C and the protein concentration was measured by Bradford's method. Cell lysates containing ~50 μg of total protein were separated by 12% SDS-PAGE and transferred to polyvinylidene difluoride (PVDF) membranes (Millipore, USA) and probed with different monoclonal and polyclonal antibodies according to the manufacturer's recommended dilution and subsequently with required secondary antibodies. Bands on the immunoblots were visualized by adding SuperSignal West Pico Chemiluminescent Substrate (Pierce, Thermo Scientific, USA) and imaged by Bio-rad ChemiDoc XRS + molecular imager. A PC-based Image Analysis program (Image Lab, Bio-rad) was used to quantify the intensity of each band. Intensity data was represented as the fold increase or decrease with respect to control bands.

2.10. Construction of luciferase reporter constructs and luciferase activity assay

For luciferase reporter assay, *pCI-neo-RL-luc* reporter vector (a generous gift from Dr. SN Bhattacharyya, IICB, Kolkata, India) was used. The wildtype or mutant Bcl-2 3′-UTRs were cloned into *pCI-neo-RL-luc* reporter vector between *Xba*I and *Not*I restriction sites, immediately downstream of the renilla luciferase gene [1]. All the luciferase constructs were sequence verified. A549-T24 cells were transiently co-transfected with renilla luciferase reporter plasmids (*pCI-neo-RL-Bcl-2-3′UTR-wt* or *pCI-neo-RL-Bcl-2-3′UTR-mut*), firefly luciferase plasmid (*pGL3-FF*) and pre-miR-16 and/or anti-sense miR-16 precursor (anti-miR-16) or pre-miR-negative control precursor RNA using Lipofectamine 2000 transfection reagent following the manufacturer's protocol. After 48 h of transfection, cells were harvested and lysed with passive lysis buffer (Promega). The luciferase activities in the cellular extracts were determined by using Promega dual luciferase reporter assay kit on a VICTOR X3 Plate Reader system (PerkinElmer). The relative luciferase activities were calculated by the ratio of renilla luc/firefly luc activity and normalized to that of the control cells and fold repression was calculated. *pGL3-FF* vector was used as the internal control.

2.11. Detection and quantification of acidic vesicular organelles (AVOs)

Acidic vesicular organelles (AVOs) were visualized after incubating cells with acridine orange (1 μg/ml) for 15 min as previously described [1]. The cytoplasm and nucleus of stained cells fluoresced bright green, whereas the acidic autophagic vacuoles fluoresced bright red. Images of AO staining were taken immediately using a fluorescence microscope (OLYMPUS IX70, Japan). To quantify the change in number of acidic vesicles (AVOs) cells were harvested from the plates by trypsinization and stained with AO (1 μg/ml) in PBS at 37 °C for 15 min, resuspended in 500 μl PBS and then analyzed immediately by flow cytometry assay.

The flow cytometric data was analyzed with CellQuest analysis software (Becton Dickinson) [1].

2.12. Labeling of autophagic vacuoles with monodansylcadaverine (MDC)

T24-miR-NC, T24-miR-17, T24-miR-16 and T24-miR-comb cells were seeded on coverslips in 35 mm culture dishes and maintained for 48 h. Cells were then incubated with 50 μM monodansylcadaverine (MDC) for 10 min at 37 °C in PBS and images were taken by fluorescence microscope (OLYMPUS IX70, Japan). Moreover, for quantitative analysis of autophagosome formation cells were incubated with 50 μM MDC for 10 min at 37 °C in PBS and were analyzed by flow cytometry.

2.13. Flow cytometric analysis for apoptotic cells

A549-T24 and H596-TxR cells, either transfected with 100 nM pre-miR-17 (T24-miR-17 and TxR-miR-17 respectively) or with 100 nM pre-miR-16 (T24-miR-16 and TxR-miR-16) or with 50 nM each of both pre-miR-17 and pre-miR-16 (T24-miR-comb and TxR-miR-comb) or with 100 nM pre-miR-negative control RNA (T24-miR-NC and TxR-miR-NC respectively) were treated with 12 nM paclitaxel for 48 h. Approximately 1×10^5 cells were then stained for 15 min at room temperature in the dark with FITC-conjugated annexin V

(1 μg/ml) and propidium iodide (PI) (0.5 μg/ml) in a Ca^{2+}-enriched binding buffer and analyzed by a two color flow cytometric assay. Annexin V and PI emissions were detected in the FL1 and FL2 channels of a FACSCalibur flow cytometer (Becton-Dickinson, USA) respectively [1,18]. The data were analyzed using CellQuest program from Becton-Dickinson.

2.14. Determination of mitochondrial membrane potential (ΔΨ)

Mitochondrial membrane potential (ΔΨ) of these miRNA transfected cells was determined using JC-1, a sensitive fluorescent probe for evaluation of ΔΨ, as previously described [1]. Briefly, T24-miR-NC, T24-miR-17, T24-miR-16 and T24-miR-comb cells were treated with 12 nM paclitaxel for 48 h. Cells were then harvested, washed with PBS, stained with 5 μM JC-1 for 30 min at 37 °C in the dark and instantly assessed for red fluorescence (JC-1) with FACSCalibur flow cytometer (Becton-Dickinson, USA).

2.15. Measurement of reactive oxygen species (ROS)

ROS levels were determined using the fluorescent dye, H2-DCFDA as previously described [1,19]. Briefly, T24-miR-NC, T24-miR-17, T24-miR-16 and T24-miR-comb cells were treated with 12 nM paclitaxel for 48 h. Cells were trypsinized and stained with 10 mM DCFH-DA for 30 min in
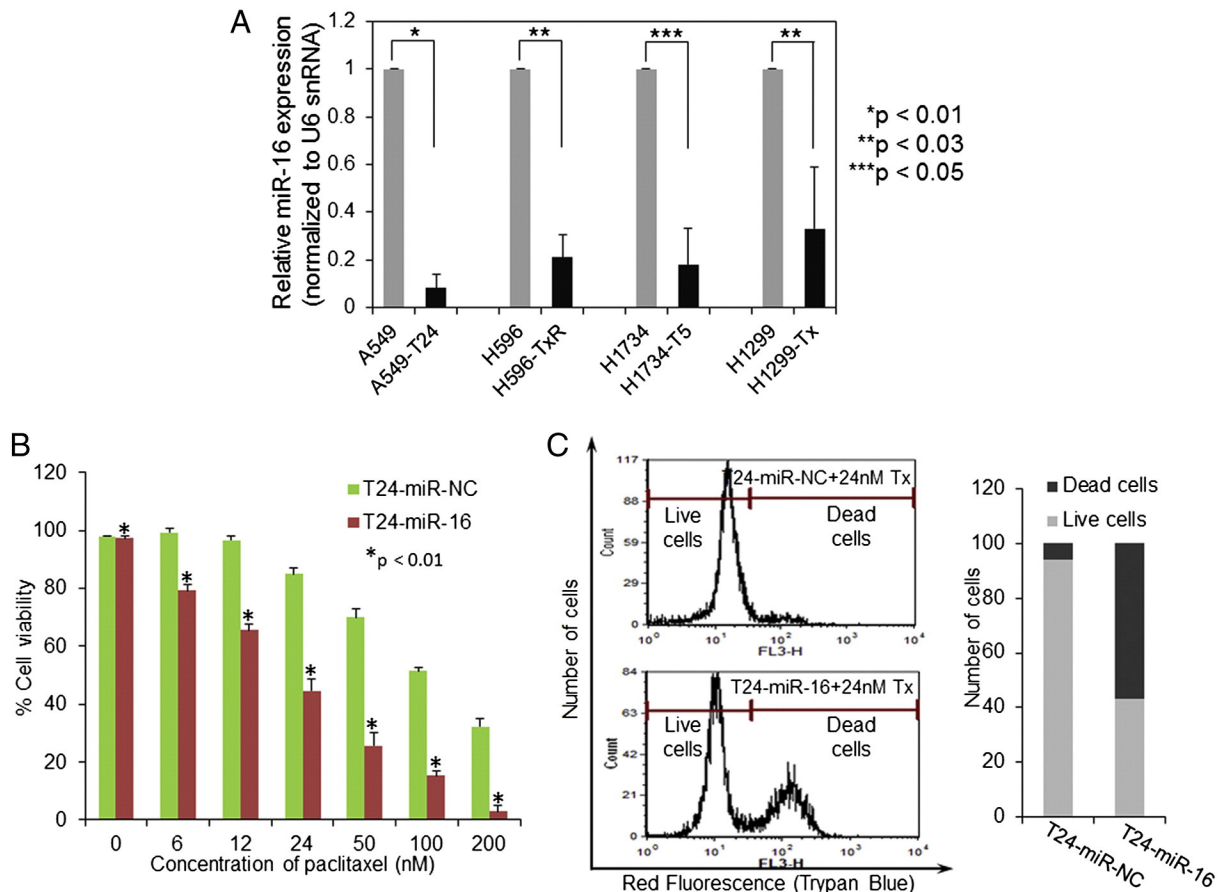

Fig. 1. miR-16 was downregulated in paclitaxel resistant lung cancer cells and miR-16 was functionally involved in the paclitaxel response to A549-T24 cells. (A) TaqMan qRT-PCR was performed to validate the expression of miR-16 in A549-T24, H596-TxR, H1734-T5 and H1299 cells compared to their respective parental cells A549, H596, H1734 and H1299 respectively. snU6 was used as an internal control and for normalization of the expression data. Columns, relative mean of expression from three independent experiments; bars, S.E. *, $p < 0.01$, **, $p < 0.03$, ***, $p < 0.05$ vs. control, n = 4. (B) A549-T24 cells were either transfected with 100 nM pre-miR-negative control (T24-miR-NC) or pre-miR-16 (T24-miR-16) precursor RNA and were seeded into 96 well plates at a density of 1×10^4 cells per well. After 24 h, cells were treated with 0–200 nM paclitaxel for another 48 h. The cell viability was measured by MTT assay. Data are presented as % of cell viability measured in cells treated with paclitaxel. Columns, mean of three independent experiments; bars, S.E. *, $p < 0.01$ vs. negative control, where n = 4. (C) Cells (T24-miR-NC and T24-miR-16) were subsequently treated with 24 nM paclitaxel for 48 h and were subjected to FACS analysis after being stained by trypan blue. Histogram represents the red fluorescence intensity (FL3-H) vs. count plots where dose dependent increase of cell death occurs. The results represent the best of data collected from three independent experiments with similar results.
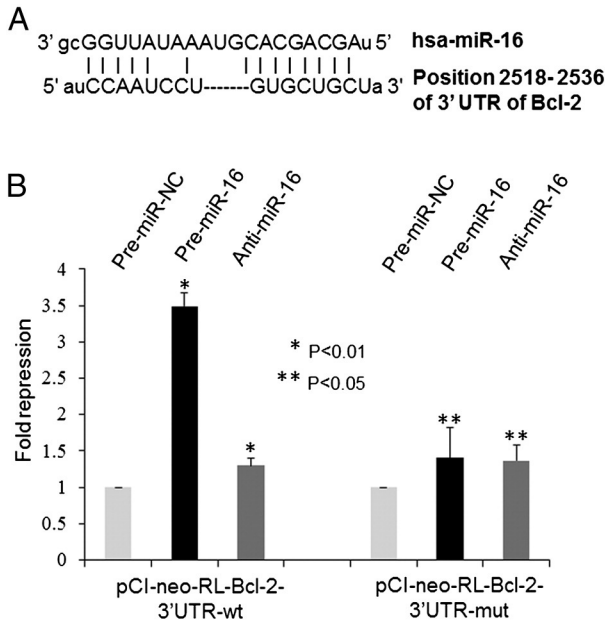
A

```
3' gcGGUUAUAAAUGCACGACGAu 5'    hsa-miR-16
        | | | | |       | | | | | | | |
5' auCCAAUCCU-------GUGCUGCUa 3'    Position 2518-2536
                                    of 3' UTR of Bcl-2
```

B

Fig. 2. miR-16 directly targets anti-apoptotic protein Bcl-2 in paclitaxel resistant A549-T24 cells. (A) Schematic representation of the 3′-UTR of human Bcl-2 transcript. Predicted miR-16 binding site was depicted. The numbers (+2518–2536) represented the nucleotides that were predicted to base pair with the miR-16 seed sequence. (B) A549-T24 cells were co-transfected with luciferase reporter plasmids with either wildtype or mutant 3′-UTR of Bcl-2 (*pCI-neo-RL-Bcl-2-3′UTR-wt* or *pCI-neo-RL-Bcl-2-3′UTR-mut*), firefly luciferase vector *pGL3-FF*, pre-miR-16 or pre-miR-negative control RNA or anti-miR-16 precursor RNA by using Lipofectamine 2000 reagent. Forty-eight hours following transfection, luciferase activity was measured as described earlier. The firefly luciferase plasmid, *pGL3-FF*, was used as an internal control. The results were represented as relative fold repression (renilla luc/firefly luc activity) compared to control cells. (*, $p < 0.05$, **, $p < 0.03$ vs. negative control, n = 4).

the dark at room temperature and the shift in the green fluorescence intensity was followed by FACSCalibur flow cytometer (Becton-Dickinson, USA) and the data was analyzed with CellQuest analysis software (Becton-Dickinson, USA).
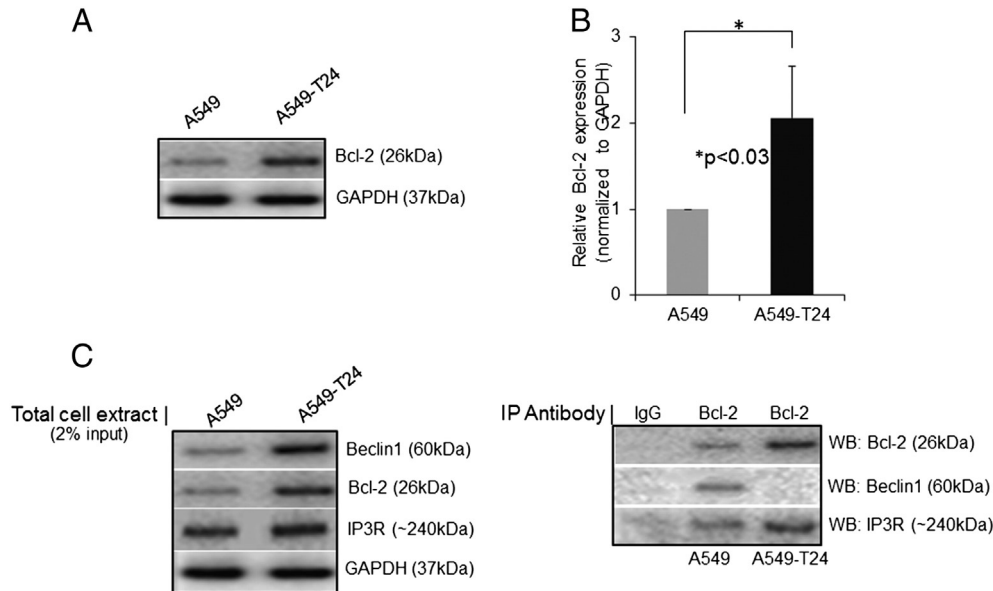
2.16. Statistical analysis

Real time PCR reactions were run in triplicate for each sample and repeated at least 3 times and the data were statistically analyzed with Student's 't-test' or Wilcoxon rank sum test. IC_{50} data from the MTT assay were analyzed with Wilcoxon rank sum test. All data were shown as the means ± S.E. (Standard error). Two measurements were statistically significant if the corresponding p value was <0.05.

3. Results

3.1. miR-16 was downregulated in various paclitaxel resistant lung cancer cell lines

In our previous report, we performed comparative miRNA microarray analysis between paclitaxel sensitive and paclitaxel resistant A549 cells to identify specific miRNAs that might be contributed in the development of paclitaxel resistance [1]. In that study we showed that miR-17 downregulation was partially involved in the development of paclitaxel resistance by upregulating Beclin-1 mediated autophagy [1]. From the differentially expressed miRNAs, we further focused on miR-16 which was significantly downregulated in the drug resistant lung cancer cells. From bioinformatic analysis, miR-16 was predicted to target anti-apoptotic gene Bcl-2 in paclitaxel resistant lung cancer cells. So, to validate the microarray data and to further extend our finding we evaluated the relative miR-16 expression levels in three other paclitaxel resistant lung cancer cell lines (H596-TxR, H1734-T5 and H1299-Tx) by TaqMan qRT-PCR and compared them with that of their paclitaxel sensitive parental cells (Fig. 1A). qRT-PCR validation of relative miR-16 levels revealed ~12.3-fold and 4.7-fold downregulation of miR-16 expression in A549-T24 and H549-TxR cell lines respectively, while H1734-T5 and H1299-Tx cells showed 5.52-fold and 3.6-fold downregulation of relative miR-16 expression level compared to their respective paclitaxel sensitive counterparts. Furthermore, as previously reported, we also observed similar downregulation of relative miR-17 expression level in all four paclitaxel resistant cell lines (A549-T24, H596-TxR, H1734-T5 and

A

B

C

Fig. 3. Expression status of Bcl-2 and Beclin-1 in A549-T24 cells compared to A549 cells and analysis of Beclin-1–Bcl-2 interaction in paclitaxel resistant A549-T24 cells compared to paclitaxel sensitive A549 cells. A549-T24 cells exhibited heightened Bcl-2 (A and B) expression compared to paclitaxel sensitive A549 cells. Columns, mean of expression from three independent experiments; bars, S.E. *, $p < 0.03$ vs. A549 control, n = 3. (C) Failure to detect an interaction of Beclin-1 and Bcl-2 in paclitaxel resistant A549-T24 cells compared to paclitaxel sensitive A549 cells. Bcl-2 immunoprecipitates from A549-T24 and A549 cells were analyzed by immunoblotting using either antibody to Beclin-1 or antibody to Bcl-2 or antibody to IP3R. The results, confirmed in three independent experiments, indicated that IP3R but not Beclin-1 was co-immunoprecipitated with Bcl-2 in A549-T24 cells while we successfully detected true interaction between Beclin-1 and Bcl-2 in parental A549 cells. Figures represent best of the data obtained from three independent experiments.
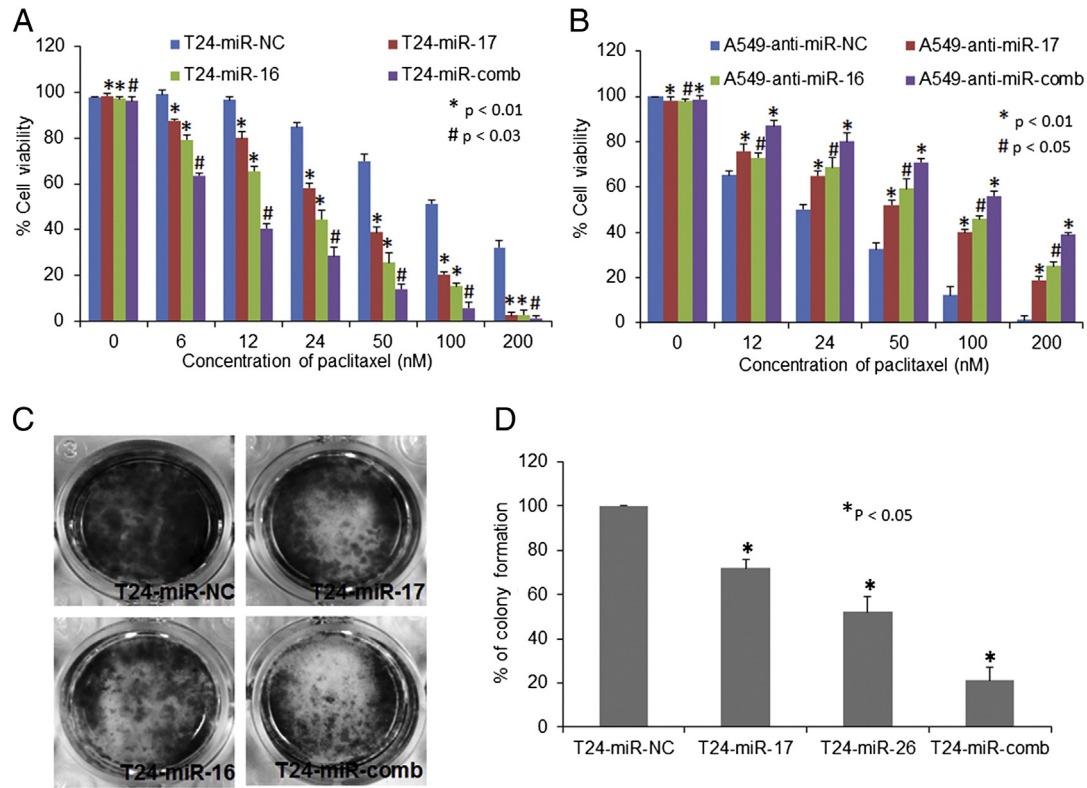
Fig. 4. Combined overexpression of both miR-16 and miR-17 potentiates paclitaxel sensitivity of paclitaxel resistant A549-T24 cells. (A) A549-T24 cells were either transfected with 100 nM pre-miR-negative control RNA (T24-miR-NC) or with 100 nM pre-miR-17 (T24-miR-17) or with 100 nM pre-miR-16 (T24-miR-16) or with 50 nM each of both pre-miR-17 and pre-miR-16 (T24-miR-comb) and were seeded into 96 well plates at a density of 1×10^4 cells per well. After 24 h, cells were treated with 0–200 nM paclitaxel for another 48 h. The cell viability was assessed by MTT assay. Data are presented as % of cell viability measured in cells treated with paclitaxel with respect to negative control. Columns, mean of three independent experiments; bars, S.E. *, $p < 0.01$ and #, $p < 0.03$ vs. negative control where n = 4. (B) A549 cells were either transfected with 100 nM anti-miR-negative control RNA (A549-anti-miR-NC) or with 100 nM anti-miR-17 (A549-anti-miR-17) or with 100 nM anti-miR-16 (A549-anti-miR-16) or with 50 nM each of both anti-miR-17 and anti-miR-16 (A549-anti-miR-comb) and were seeded into 96 well plates at a density of 1×10^4 cells per well. After 24 h, cells were treated with 0–200 nM paclitaxel for another 48 h. Cell viability was determined by MTT assay method and was expressed as a percentage of negative control. Columns, mean of three independent experiments; bars, S.E. *, $p < 0.01$ and #, $p < 0.05$ vs. negative A549 control where n = 4. (C) Colony formation assay. T24-miR-NC, T24-miR-17, T24-miR-16 and T24-miR-comb cells were seeded in triplicate in 6 well plates at a density of 1000 cells per well. The cells were then treated with 12 nM paclitaxel for 48 h. Then fresh culture media was added to each well and the cells were allowed to grow for 15 days at 37 °C, 5% CO_2 with media changes in every 3–4 days until colonies were visible by the eye. The resultant cell colonies were fixed and then stained with 0.5% crystal violet solution. The stained colonies were imaged by Bio-rad ChemiDoc XRS + molecular imager. The results represent the best of data collected from three independent experiments with similar results. (D) Colony formation was quantitated by dissolving stained cells in Sorenson's buffer for colorimetric reading of absorbance at 550 nm. Columns, mean of three independent experiments; bars, S.E. *, $p < 0.05$ vs. negative control where n = 4.

H1299-Tx) compared to their respective paclitaxel sensitive variants (Fig. 1B) [1]. These data also suggested that downregulation of miR-16 and miR-17 following paclitaxel resistance was not limited to a particular cell line.

3.2. Sensitivity to paclitaxel was modulated by over-expression of miR-16 in vitro

To investigate whether miR-16 overexpression could sensitize A549-T24 cells to paclitaxel, cell viability of A549-T24 was measured by transfecting pre-miR-16 (T24-miR-16) or pre-miR-negative control RNA (T24-miR-NC). It was observed that compared to the negative control (T24-miR-NC), overexpression of miR-16 significantly sensitized the A549-T24 cells to paclitaxel (Fig. 1B). Moreover, to extend our finding, we repeated this experiment with H596-TxR cells and we found that compared to the negative control (TxR-miR-NC), TxR-miR-16 cells exhibited much lower cell viability when treated with increasing concentrations of paclitaxel (Fig. S1B).

The cyto-toxic effects of miR-16 overexpression and subsequent paclitaxel treatment were further evaluated by trypan blue dye exclusion assay using flow cytometer with A549-T24 cells (Fig. 1C). Fig. 1C showed that with miR-16 overexpression and subsequent paclitaxel treatment (24 nM) for 48 h resulted in the significant reduction of residual viability of T24-miR-16 cells compared to T24-miR-NC cells.

3.3. miR-16 directly targeted anti-apoptotic protein Bcl-2 in paclitaxel resistant lung cancer cells

Bioinformatic prediction indicated that miR-16 might target anti-apoptotic protein Bcl-2. To validate whether miR-16 directly binds to the 3′-UTR region of Bcl-2 mRNA, we constructed 3′-UTR reporters of Bcl-2 containing putative miR-16 binding site (Fig. 2A). Co-transfection of these reporter constructs with pre-miR-16 in A549-T24 cells resulted in the significant repression of relative renilla luciferase activity (Fig. 2B) as compared to the negative control (A549-T24 cells transfected with luciferase reporter and pre-miR-negative control RNA). Moreover, we also prepared mutant 3′-UTR reporter of Bcl-2 with mutated miR-16 binding sites. When A549-T24 cells were co-transfected with this mutant construct along with pre-miR-16, no significant repression of relative luciferase activity compared to the negative control was observed (Fig. 2B). All these results collectively confirmed that Bcl-2 was the direct target of miR-16 in A549-T24 cells.

3.4. The level of miR-16 was inversely correlated with relative Bcl-2 expression in paclitaxel resistant lung cancer cells

Previous studies suggested that anti-apoptotic protein Bcl-2 expression is regulated by miR-16 [20–23]. Moreover, in this study we observed that miR-16 directly interacted with the 3′-UTR region of Bcl-2

mRNA (Fig. 2). As paclitaxel resistant lung cancer cells exhibited reduced expression of miR-16, we checked the cellular status of Bcl-2 in A549-T24 cells and compared it with that of A549 cells. We found that paclitaxel resistant lung cancer cells exhibited increased expression of Bcl-2 (Fig. 3A). Estimation of the relative mRNA level of Bcl-2 (Fig. 3B) by qRT-PCR indicated ~2 fold upregulation of Bcl-2 mRNA level in A549-T24 cells compared to parental A549 cells. We also observed similar upregulation in the expression level of Bcl-2 in H596-TxR cells by Western blotting and qRT-PCR analysis (Fig. S2A and B).

3.5. Upregulation of Bcl-2 did not impede Beclin-1 mediated autophagy in paclitaxel resistant lung cancer cells

It has been previously reported that Bcl-2 interacts with Beclin-1 and thereby inhibits autophagy by downregulating Beclin-1 expression [24, 25]. But here we observed that paclitaxel-resistant lung cancer cells exhibited increase level of Bcl-2 expression and higher level of autophagy with increased expression of Beclin-1 compared to parental cells (Figs. 3C and S2C). This appeared to be in conflict with the previous reports describing Bcl-2 as an antagonist of autophagy [24]. Therefore, we checked the interaction of Bcl-2 and Beclin-1 in paclitaxel resistant lung cancer cells. In a co-immunoprecipitation experiment we were unable to detect any interaction between Bcl-2 and Beclin-1 (Figs. 3C and S2C) although we successfully detected co-immunoprecipitated inositol 1,4,5-triphosphate receptor (IP3R) with Bcl-2 (Figs. 3C and S2C) as

previously described [26–28]. This was observed both in the case of A549-T24 and H596-TxR cells indicating that the inhibition of Beclin-1 and Bcl-2 interactions following paclitaxel resistance was not cell line specific. Altogether these results were in accordance with several recent reports showing that Bcl-2 does not inhibit autophagy but rather facilitates the cells to undergo autophagy by inhibiting apoptosis [29–31].

3.6. Combined overexpression of miR-16 and miR-17 potentiates paclitaxel sensitivity of paclitaxel resistant lung cancer cells

If resistance to paclitaxel is causally related to the downregulation of miR-17 [1] and miR-16 in lung cancer cells (Figs. 1A and S1A), then modulating the expression levels of both miR-17 and miR-16 simultaneously should alter paclitaxel sensitivity. Previously, we showed that ectopic expression of miR-17 into paclitaxel resistant lung cancer cells and subsequent treatment with paclitaxel sensitized the cells to paclitaxel [1]. Moreover, here in this study, we showed that forced expression of miR-16 and subsequent paclitaxel treatment significantly sensitized paclitaxel resistant lung cancer cells to paclitaxel (Figs. 1B–C and S1B). So we hypothesized that since individual overexpression of either miR-16 or miR-17 and subsequent paclitaxel treatment were capable of modulating paclitaxel sensitivity of the drug resistant cells, combined overexpression of both miRNAs would potentiate paclitaxel sensitivity. So, we investigated the combined role of miR-16 and miR-
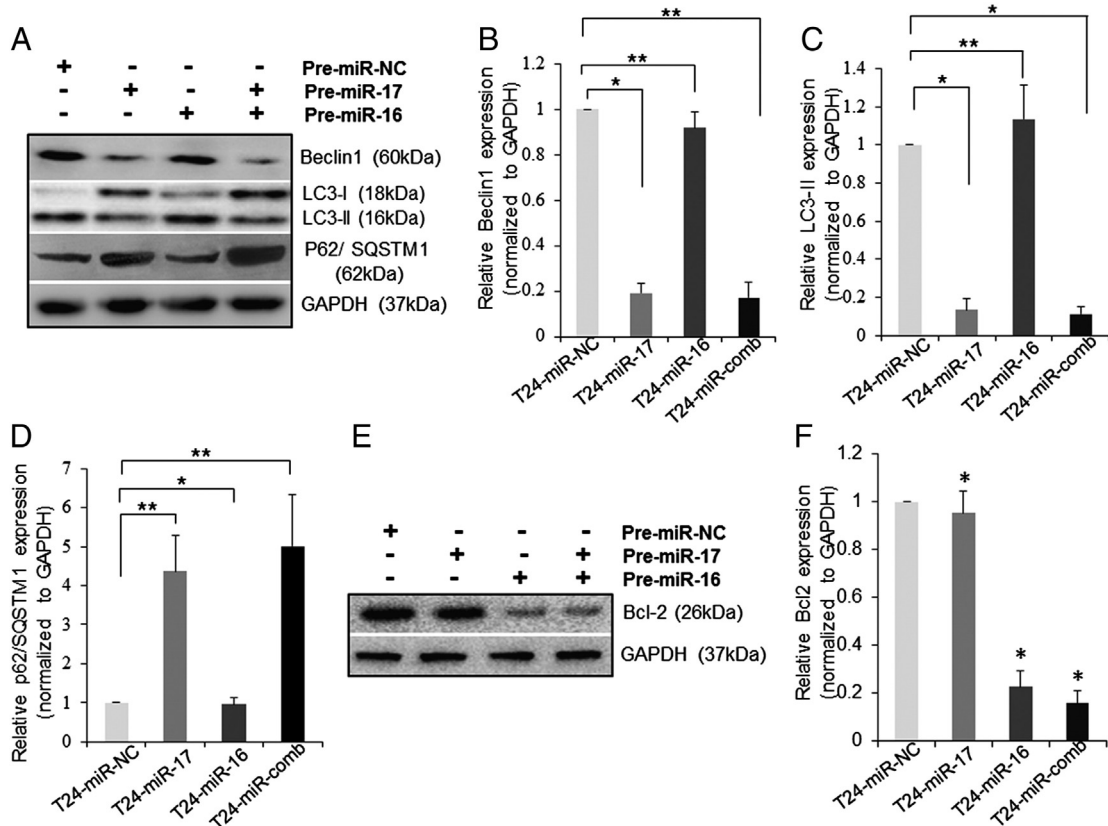

Fig. 5. miR-16 and miR-17 modulate the expression of Beclin-1 and Bcl-2 in paclitaxel resistant A549-T24 cells, respectively. (A) A549-T24 cells were either transfected with 100 nM pre-miR-negative control RNA (T24-miR-NC) or with 100 nM pre-miR-17 (T24-miR-17) or with 100 nM pre-miR-16 (T24-miR-16) or with 50 nM each of both pre-miR-16 and pre-miR-17 precursor RNA (T24-miR-comb) and 48 h following transfection cell lysates were prepared for Western blotting with antibody against Beclin-1, MAP-LC3B, p62 and GAPDH (loading control). (B–D) Relative expression levels of Beclin-1, LC3-II and p62 mRNAs were analyzed by qRT-PCR for the same transfected samples. Expression of GAPDH mRNA was used as endogenous reference and also for normalization of results. Columns, mean relative expression from three independent samples; bars, S.E. *, $p < 0.01$, **, $p < 0.03$ vs. negative control, where n = 4. (E) A549-T24 cells were either transfected with 100 nM pre-miR-negative control RNA (T24-miR-NC) or with 100 nM pre-miR-17 (T24-miR-17) or with 100 nM pre-miR-16 (T24-miR-16) or with 50 nM each of both pre-miR-16 and pre-miR-17 precursor RNA (T24-miR-comb) and 48 h following transfection cell lysates were prepared for Western blotting with antibody against Bcl-2 and GAPDH (loading control). (F) Relative expression level of Bcl-2 mRNAs was analyzed by qRT-PCR for the same transfected samples. The results were normalized to GAPDH expression. Columns, mean relative expression from three independent samples; bars, S.E. *, $p < 0.03$ vs. negative control, where n = 4.

17 overexpression in paclitaxel induced cytotoxicity in two paclitaxel resistant lung cancer cell lines (A549-T24 and H596-TxR). Moreover to compare the result of combined miRNA overexpression with that of single miRNA overexpression we showed them in parallel. We overexpressed A549-T24 or H596-TxR cells with miR-16 and miR-17 simultaneously and subsequently treated with varying doses of paclitaxel for 48 h and determined cell viability by MTT assay. We observed that irrespective of the cell type, combined overexpression of miR-16 and miR-17 followed by treatment with paclitaxel significantly sensitized the paclitaxel resistant lung cancer cells to a lower dose of paclitaxel (Figs. 4A and S3A). For example, when miR-17 was overexpressed, the IC_{50} values for 48 h paclitaxel treatment were 29.8 ± 1.5 nM for A549-T24 cells and 41 ± 2 nM for H596-TxR cells. For overexpression of miR-16, IC_{50} values were 21.5 ± 1.7 nM for A549-T24 cells and 34 ± 2.5 nM in H596-TxR cells for 48 h paclitaxel exposure. Interestingly, IC_{50} values were reduced significantly to 10.9 ± 0.42 nM for A549-T24 cells and 19 ± 2.5 nM for H596-TxR cells when cells were co-transfected with both pre-miR-16 and pre-miR-17 and subsequently treated with paclitaxel for 48 h.

Moreover, to complement these results, we transfected paclitaxel sensitive parental lung cancer cells (both A549 and H596 cells) either with anti-miR-17 or with anti-miR-16 or with both anti-miRNAs simultaneously and measured cell viability in the presence of paclitaxel (0–200 nM) with the expectation that these treatments would result in acquisition of the resistant phenotype. We observed that as expected when A549 or H596 cells were simultaneously transfected with both antisense miR-16 (anti-miR-16) and antisense miR-17 (anti-miR-17) they exhibited maximum tolerance to paclitaxel compared to the cells transfected with individual anti-miRNA (Figs. 4B and S3B).

3.7. Combined overexpression of both miR-16 and miR-17 reduced the colony forming ability of A549-T24 cells

Cultured A549-T24 cells were either transfected with pre-miR-negative control RNA (T24-miR-NC) or with pre-miR-16 (T24-miR-16) or with pre-miR-17 (T24-miR-17) or with both pre-miRNAs (T24-miR-comb) and 24 h following transfection cells were treated with 12 nM paclitaxel for another 48 h. Thereafter, cells were maintained
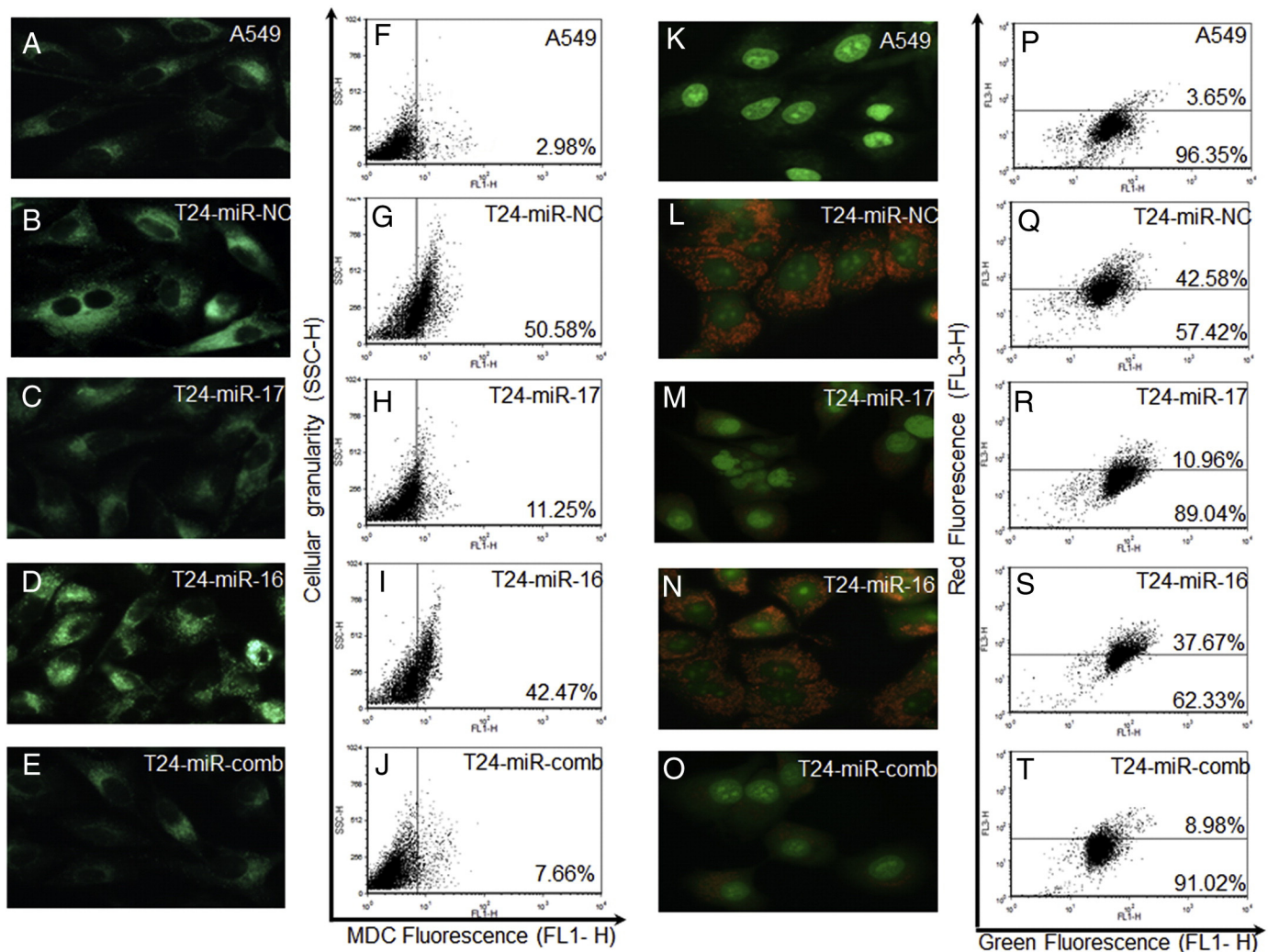

Fig. 6. Detection of autophagy following combined overexpression of miR-16 and miR-17 into paclitaxel resistant A549-T24 cells. (B–E) The fluorescence image of MDC fluorescence of punctuates (autophagosome) following overexpression of A549-T24 cells with either miR-16 or miR-17 or miR-16 and miR-17 in combination. A549-T24 cells were either transfected with 100 nM pre-miR-negative control RNA (T24-miR-NC) (B) or with 100 nM pre-miR-17 (T24-miR-17) (C) or with 100 nM pre-miR-16 (T24-miR-16) (D) or with 50 nM each of both pre-miR-16 and pre-miR-17 precursor RNA (T24-miR-comb) (E) and 48 h following transfection cells were labeled with MDC, images were taken by fluorescence microscope (OLYMPUS IX70, Japan). MDC staining of A549 served as the control (A). (F–J) Flow cytometric quantitation of change in autophagic vacuole formation in A549 (F), T24-miR-NC (G), T24-miR-17 (H), T24-miR-16 (I) and T24-miR-comb (J) cells respectively following staining with MDC. (L–O) T24-miR-NC (L), T24-miR-17 (M), T24-miR-16 (N) and T24-miR-comb (O) cells were stained with A.O for AVO observation under fluorescence microscope. A.O staining of A549 was used as control (K). (P–T) To quantitate change in % of cells developing AVO following miRNA overexpression into A549-T24 cells, flow-cytometric estimation of AVOs was done in A549 (P), T24-miR-NC (Q), T24-miR-17 (R), T24-miR-16 (S) and T24-miR-comb (T) cells respectively following A.O staining. A.O staining of A549 cells was used as control.

for another 15 days with triweekly change in media and then stained with crystal violet and the images of the resultant cell colonies were taken (details in Materials and methods section). We found that when A549-T24 cells were co-overexpressed with both miR-16 and miR-17 and treated with 12 nM paclitaxel (IC_{50} dose) for 48 h, cells exhibited much lower colony formation (Fig. 4C). For example, when A549-T24 cells were overexpressed with miR-17 or miR-16 or miR-16 and miR-17 in combination and treated with 12 nM paclitaxel for 48 h, % colony formation abilities were 70 ± 3.98%, 52 ± 6.56% and 20 ± 5.96%, respectively, with respect to that of the negative control (T24-miR-NC) (Fig. 4D).

3.8. Co-overexpression of miR-16 and miR-17 led to downregulation of both Bcl-2 and Beclin-1 expressions respectively in paclitaxel resistant lung cancer cells

To functionally validate the combined role of miR-16 and miR-17 downregulation in paclitaxel resistance, we overexpressed A549-T24 cells either with pre-miR-16 or with pre-miR-17 or with both miRNAs and examined the expression of both Beclin-1 and Bcl-2. We found that compared to the negative control (T24-miR-NC) when A549-T24 cells were overexpressed with miR-17 (T24-miR-17) or miR-17 and miR-16 in combination (T24-miR-comb), a marked decrease in Beclin-1 expression level was observed (Fig. 5A, first blot and Fig. 5B). We

also evaluated the cellular expression levels of two other autophagic marker proteins, MAP-LC3-II and p62/SQSTM1 downstream to Beclin-1. We found that overexpression of miR-17 or a combination of miR-16 and miR-17 into A549-T24 cells resulted in accumulation of p62/SQSTM1 (Fig. 5A, third blot and Fig. 5D) and reduction in LC3-I to LC3-II conversion (Fig. 5A, second blot and Fig. 5C) indicating inhibition of autophagy. To extend our findings we tested the mRNA expression status of these autophagy related genes (i.e. Beclin-1, LC3-II and p62/SQSTM1) in H596-TxR cells following overexpression with either miR-17 or with miR-16 or with both miRNAs in combination. Overexpression of miR-17 or miR-17 and miR-16 in combination in H596-TxR cells caused significant downregulation of Beclin-1 and LC3-II expressions with a marked increase in p62/SQSTM1 mRNA level (Fig. S4A and B).

Furthermore, forced expression of miR-16 or a combination of miR17 and miR-16 into A549-T24 cells resulted in the concordant downregulation of cellular Bcl-2 protein level (Fig. 5E). Investigation of relative mRNA expression levels of Bcl-2 in those miRNA transfected cells revealed marked downregulation of Bcl-2 mRNA expression in T24-miR-16 and T24-miR-comb cells as compared to the negative control (Fig. 5F) and thereby confirming Bcl-2 expression to be negatively regulated by miR-16 in vitro. However, overexpression of miR-17 did not significantly affect the status of Bcl-2 (Fig. 5E and F) indicating that miR-17 had no influence on Bcl-2 expression in A549-T24
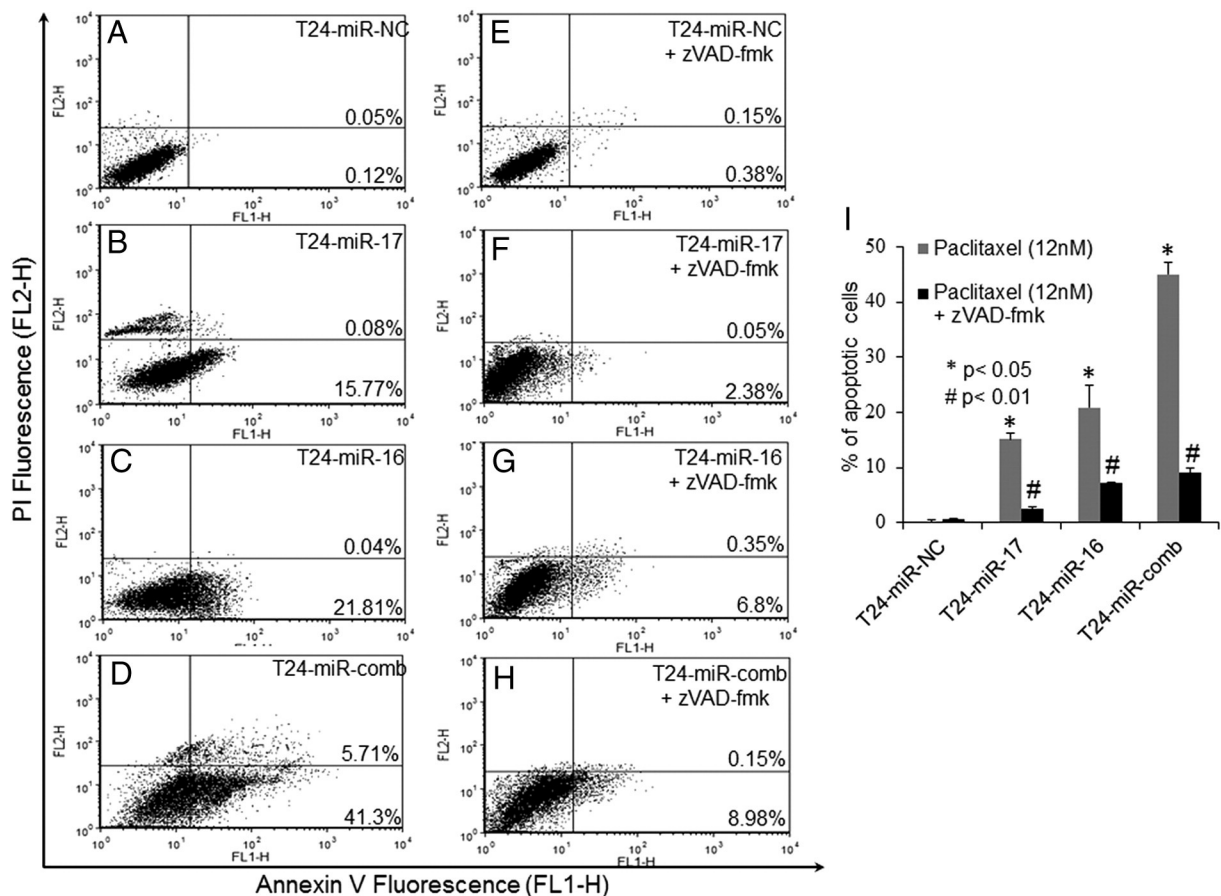

Fig. 7. Combined overexpression of miR-16 and miR-17 and subsequent paclitaxel treatment potentiates cellular apoptosis in A549-T24 cells via mitochondrial caspase dependent pathway. Annexin V–FITC/PI assay for determination of apoptosis of pre-miRNA transfected and 12 nM paclitaxel treated A549-T24 cells using flow cytometer. (A–D) A549-T24 cells were either transfected with 100 nM pre-miR-negative control RNA (T24-miR-NC) (A) or with 100 nM pre-miR-17 (T24-miR-17) (B) or with 100 nM pre-miR-16 (T24-miR-16) (C) or with 50 nM each of both pre-miR-16 and pre-miR-17 (T24-miR-comb) (D) and 24 h following transfection cells were incubated with paclitaxel (12 nM) for 48 h. Cells were harvested and stained with annexin V–FITC and PI. The percentage of early apoptotic cells located in the lower right quadrant (annexin V–FITC positive/PI negative cells), as well as late apoptotic cells located in the upper right quadrant (annexin V–FITC positive/PI positive cells) were determined. (E–H) T24-miR-NC (E), T24-miR-17 (F), T24-miR-16 (G) and T24-miR-comb (H) cells were pre-treated with pan-caspase inhibitor zVAD-fmk followed by treatment with paclitaxel for 48 h and then analyzed for apoptosis by annexin V–FITC/PI staining and flow cytometry. (I) Percentage of apoptotic cells (annexin V-positive cells) was plotted against different sample sets. Columns, mean cell count of annexin V positive population from three independent samples; bars, S.E. *, $p < 0.05$, #, $p < 0.01$ vs. negative control where n = 4.

cells. We also tested the status of Bcl-2 in H596-TxR cells following combined overexpression of miR-17 and miR-16. Similar downregulation of Bcl-2 expression level was observed when H596-TxR cells were overexpressed with either miR-16 or miR-17 and miR-16 in combination (Fig. S4C and D). Moreover, these results also collectively indicated that overexpression of miR-16 did not interfere with the expression of Beclin-1 and overexpression of miR-17 did not modulate relative Bcl-2 expression indicating that these two miRNAs mediate their effects through two different pathways.

3.9. Co-overexpression of miR-16 and miR-17 reduced cellular autophagy in A549-T24 cells

Chemotherapeutic agent paclitaxel exerts its cytotoxic effect by inducing apoptosis [32]. However, cancer cells trigger multiple survival pathways to overcome the adverse effects of chemotherapy. In recent years, autophagy has emerged as one of the most widely studied survival pathways which help the cancer cells to survive and escape from chemotherapy induced cytotoxicity [7,18,33,34]. Paclitaxel is known to induce autophagy in cancer cells [7,8,35]. Previous reports show that paclitaxel resistant lung cancer cells exhibit increased level of autophagy and miR-17 downregulation contributes to this upregulation of

cytoprotective autophagy which helps lung cancer cells to withstand cytotoxic effects of paclitaxel and develop paclitaxel resistance [1,8]. Here in this report we were interested to see whether combined overexpression of miR-17 and miR-16 could inhibit autophagosome formation in A549-T24 cells. We used two different stains for detecting autophagic vacuoles, monodansylcadaverine (MDC) which accumulates in matured autophagic vacuoles but not in early endosomal compartments which are acidic in nature and gives a green fluorescence or acridine-orange (A.O) which binds to autophagic acidic vacuoles (AVOs) and thereby marks AVOs by the appearance of red fluorescence. From fluorescence microscopic examination we found that compared to the negative control (T24-miR-NC) (Fig. 6B and L), when A549-T24 cells were overexpressed with pre-miR-17 (T24-miR-17) (Fig. 6C and M) or with the combination of pre-miR-17 and pre-miR-16 (T24-miR-comb) (Fig. 6E and O), autophagosome formation was markedly reduced. Under similar conditions paclitaxel sensitive parental A549 cells displayed almost no fluorescent vesicles (Fig. 6A and K). This was observed both in the case of MDC stained and A.O stained cells. Moreover, we also observed that overexpression of miR-16 into A549-T24 cells did not significantly affect the autophagosome formation as T24-miR-16 cells exhibited the presence of significant amount of AVOs (Fig. 6D and N). Furthermore, we also performed flow cytometry analysis of
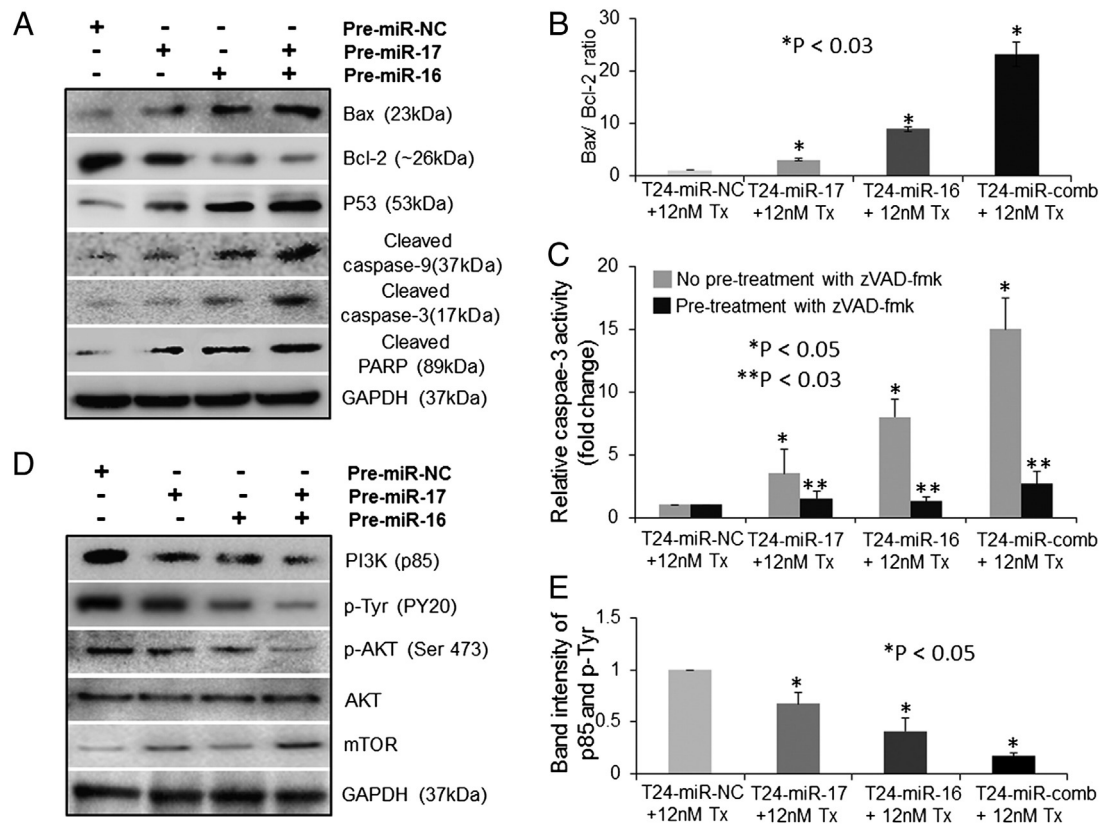

Fig. 8. Combined overexpression of miR-16 and miR-17 and subsequent paclitaxel (12 nM) treatment resulted in activation of caspase 3 mediated mitochondrial apoptotic pathway with simultaneous inhibition of PI3K/Akt/mTOR pathway in paclitaxel resistant A549-T24 cells. (A) Western Blot analysis of different apoptotic and anti-apoptotic marker proteins. A549-T24 cells were either transfected with 100 nM pre-miR-negative control RNA (T24-miR-NC) or with 100 nM pre-miR-17 (T24-miR-17) or with 100 nM pre-miR-16 (T24-miR-16) or with 50 nM each of both pre-miR-16 and pre-miR-17 precursor RNA (T24-miR-comb) and treated with 12 nM paclitaxel for 48 h. Following cell lysis, equal amounts of proteins were subjected to Western Blot analysis to detect the change in expression of different pro- and anti-apoptotic proteins (Bax, Bcl-2, P53, cleaved caspase 9, cleaved caspase 3 and cleaved PARP). GAPDH served as the loading control. (B) Estimation of Bax/Bcl-2 ratio in T24-miR-NC, T24-miR-17, T24-miR-16 and T24-miR-comb cells following paclitaxel treatment (12 nM) for 48 h. The change of expression ratio of Bax/Bcl-2 was calculated by densitometric scanning of band intensities. Columns, relative mean ratio of band intensities; bars, S.E. *, $p < 0.03$ vs. negative control where n = 3. (C) Measurement of caspase 3 activity in the presence and absence of zVAD-fmk in T24-miR-NC, T24-miR-17, T24-miR-16 and T24-miR-comb cells following treatment with 12 nM paclitaxel for 48 h. Columns, relative caspase 3 activity; bars, S.E. *, $p < 0.05$, **, $p < 0.03$ vs. negative control where n = 3. (D) Combined overexpression of miR-16 and miR-17 resulted in the marked inhibition of PI3K/Akt/mTOR pathway in A549-T24 cells. T24-miR-NC, T24-miR-17, T24-miR-16 and T24-miR-comb cells were treated with 12 nM paclitaxel for 48 h. Following cell lysis, equal amounts of proteins were immunoprecipitated by antibody against the regulatory p85 subunit of PI3K and then p85 immunoprecipitates were immunoblotted with anti-phosphotyrosine (p-Tyr) antibody and anti-p85 antibody to check the total and phosphorylated amount of PI3K. The expression status of phosphorylated (at Ser473 residue), total Akt kinase and mTOR in paclitaxel treated T24-miR-NC, T24-miR-17, T24-miR-16 and T24-miR-comb cells was measured by Western blotting. (E) The change of expression of p85 and p-Tyr was calculated by densitometric scanning of band intensity and plotted against respective samples. Columns, band intensities; bars, S.E. *, $p < 0.05$ vs. negative control where n = 4.

these samples after staining them with either MDC or AO for the quantitation of AVOs and we found similar results (Fig. 6F–J and P–T). These results along with the other results collectively suggested that miR-17 and miR-16 mediate their effects via two independent pathways i.e. they don't have a common target in paclitaxel resistant lung cancer cells.

3.10. Co-overexpression of miR-16 and miR-17 markedly sensitized the paclitaxel resistant lung cancer cells by promoting paclitaxel induced apoptosis

Since co-overexpression of miR-16 and miR-17 sensitized the paclitaxel resistant lung cancer cells to a much lower dose of paclitaxel (Figs. 4A and S3A), we were interested to investigate whether this increase in cytotoxicity was the result of increase in apoptosis in both A549-T24 and H596-TxR cells. T24-miR-NC and TxR-miR-NC or T24-miR-17 and TxR-miR-17 or T24-miR-16 and TxR-miR-16 or T24-miR-comb and TxR-miR-comb cells were treated with 12 nM paclitaxel for another 48 h. Then the cells were fixed and labeled with FITC–annexin V antibody and propidium iodide (PI) and subjected to a two color flow cytometric assay. Flow cytometric analysis revealed that % of annexin V and annexin V/PI positive cells increased significantly in the cells

overexpressing both miRNAs (T24-miR-comb and TxR-miR-comb) than the cells overexpressing any of the individual miRNAs (miR-17 or miR-16 individually) or the negative control RNA (T24-miR-NC and TxR-miR-NC) (Figs. 7A–D and S4A–D). For example, compared to the negative control (T24-miR-NC and TxR-miR-NC), when the cells were overexpressed either with miR-17 (T24-miR-17 and TxR-miR-17) or with miR-16 (T24-miR-16 and TxR-miR-16) individually, the numbers of apoptotic cells were 16% (T24-miR-17), 9.5% (TxR-miR-17) and 22% (T24-miR-16), and 15.5% (TxR-miR-16). However when the cells were overexpressed with both miRNAs in combination and subsequently treated with 12 nM paclitaxel for 48 h, % of apoptotic cells increased to 47% (T24-miR-comb) and 34% (TxR-miR-comb) indicating significant enhancement of cellular apoptosis (Figs. 7A–D and S4A–D). Moreover, when these miRNA transfected cells were pre-treated with the pan-caspase inhibitor zVAD-fmk for 2 h before treatment with 12 nM paclitaxel for 48 h, the percentage of cells undergoing apoptosis reduced significantly (Fig. 7A–D compared to Fig. 7E–H and Fig. S4A–D compared to Fig. S5E–H), suggesting that this increase in apoptosis induced by combined overexpression of miR-17 and miR-16 followed by treatment with paclitaxel was caspase dependent.

Furthermore, the inhibitory effect of pan-caspase inhibitor zVAD-fmk on apoptosis of A549-T24 cells following combined overexpression
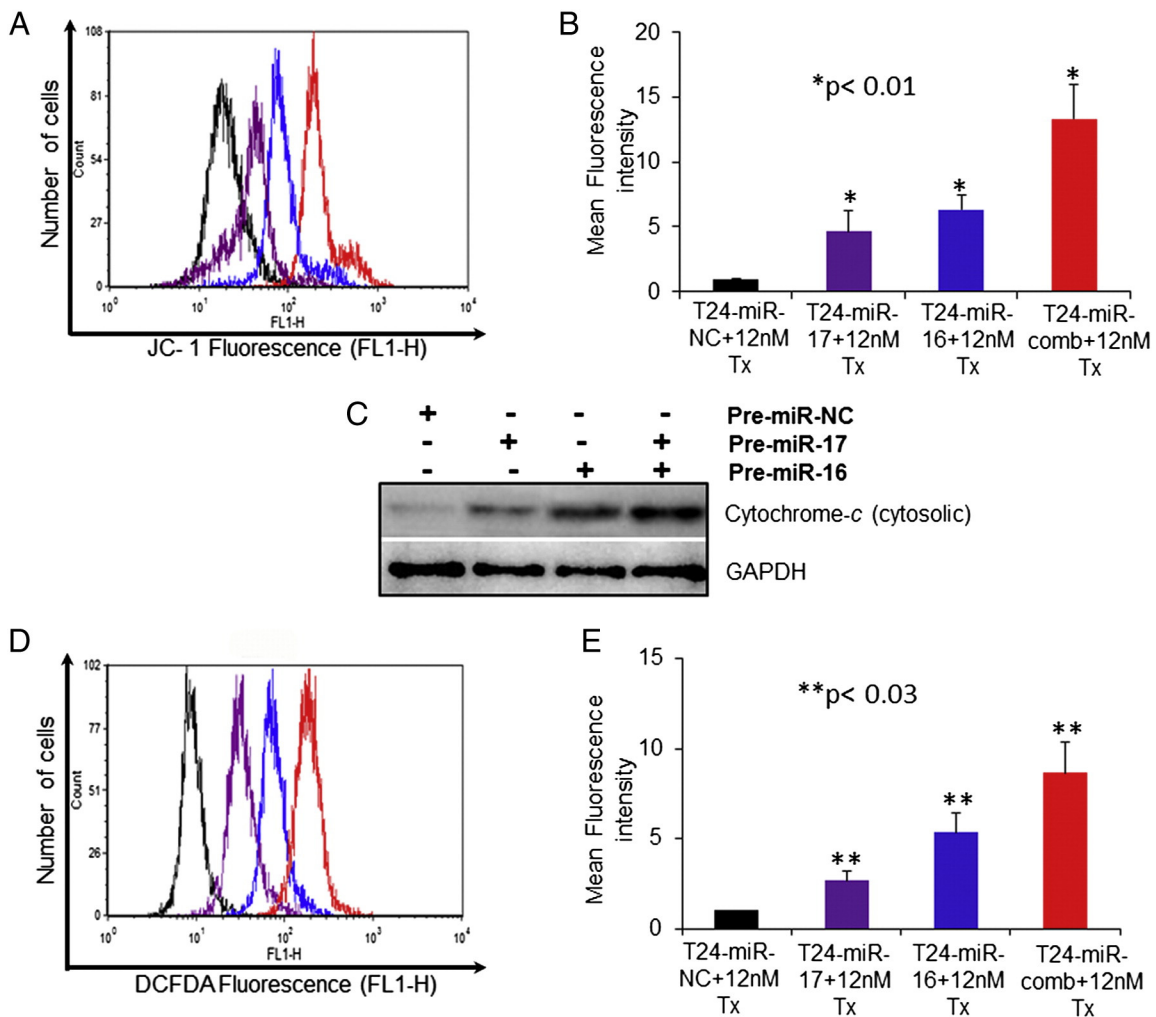

Fig. 9. Simultaneous inhibition of Beclin-1 mediated autophagy by miR-17 overexpression and downregulation of anti-apoptotic protein Bcl-2 expression by miR-16 overexpression and subsequent paclitaxel treatment induced collapse of mitochondrial membrane potential and stimulated ROS generation in A549-T24 cells. (A-B) T24-miR-NC, T24-miR-17, T24-miR-16 and T24-miR-comb cells were treated with 12 nM paclitaxel for 48 h. Then the treated-cells were harvested, PBS washed and finally stained with JC-1 and analyzed by flow cytometer. Histogram represents enhancement of green fluorescence (FL2-H) intensity vs. cell count plots where mitochondrial membrane potential decreases following combined overexpression of miR-17 and miR-16 and subsequent paclitaxel treatment. (C) Western Blot analysis to detect the release of the cytochrome-c in the cytosol from the mitochondria in T24-miR-NC, T24-miR-17, T24-miR-16 and T24-miR-comb cells following paclitaxel treatment for 48 h. GAPDH served as the loading control. (D–E) Evaluation of ROS levels in T24-miR-NC, T24-miR-17, T24-miR-16 and T24-miR-comb cells following paclitaxel treatment for 48 h. ROS generation was estimated by staining of the cells with H2-DCFDA dye and flow cytometry.
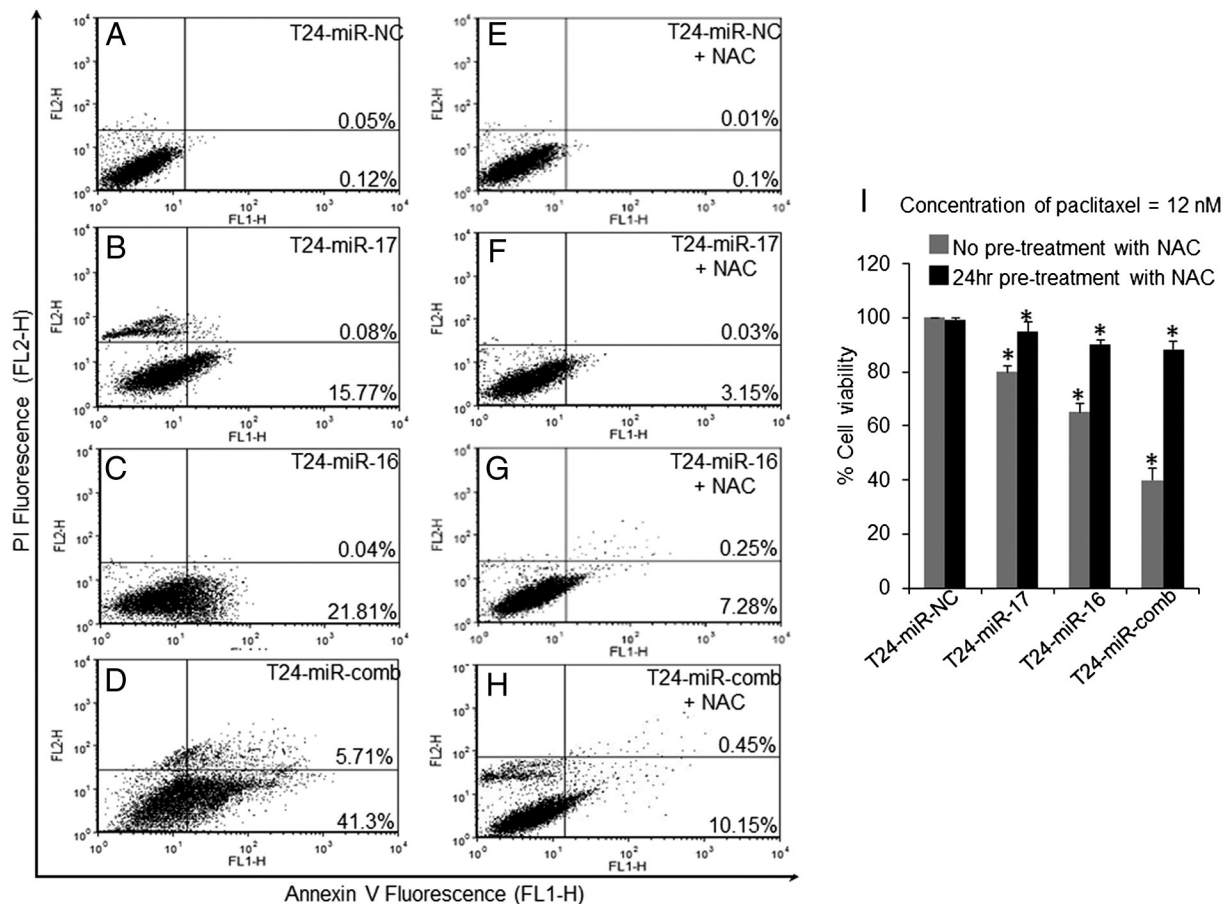
Fig. 10. Amelioration of paclitaxel induced cytotoxicity following combined overexpression of miR-16 and miR-17 in A549-T24 cells by N-acetyl-L-cysteine (NAC). A549-T24 cells were either transfected with 100 nM pre-miR-negative control RNA (T24-miR-NC) or with 100 nM pre-miR-17 (T24-miR-17) or with 100 nM pre-miR-16 (T24-miR-16) or with 50 nM each of both pre-miR-16 and pre-miR-17 precursor RNA (T24-miR-comb). (E–H) Cells were pre-incubated with 1 mM NAC for 4 h and then treated with 12 nM paclitaxel for 48 h. Finally after labeling with annexin V and PI for apoptosis assay, the cells were analyzed by flow cytometer. (A–D) T24-miR-NC (A), T24-miR-17 (B), T24-miR-16 (C) and T24-miR-comb (D) cells were treated with 12 nM paclitaxel for 48 h. Cells were harvested, stained with annexin V–FITC and PI and analyzed by flow cytometer. The percentages of early and late apoptotic cells were determined. (I) T24-miR-NC, T24-miR-17, T24-miR-16 and T24-miR-comb cells were pre-incubated with 1 mM NAC for 4 h and then treated with 12 nM paclitaxel for 48 h. Cell viability was measured by MTT assay and was expressed as the percentage of negative control. Columns, mean of cell viability from three independent experiments; Columns, mean cell viability from three independent experiments; bars, S.E. *, $p < 0.01$ vs. negative control where n = 4.

of miR-16 and miR-17 and subsequent paclitaxel treatment (Fig. 7) intrigued us to investigate the status of major protein components of mitochondrial apoptotic pathway by Western blotting. We found that when A549-T24 cells were jointly overexpressed with miR-16 and miR-17 and subsequently treated with 12 nM paclitaxel for 48 h, a significant increase in Bax (pro-apoptotic)/Bcl-2 (anti-apoptotic) ratio (Fig. 8A and B) was observed. Moreover, we observed that co-overexpression of miR-16 and miR-17 resulted in increase in the p53 level and increase in the amount of a cleaved caspase-3 (19 kDa) as well as cleaved poly (ADP-ribose) polymerase (PARP) (Fig. 8A).

Moreover, to extend our finding we also measured mRNA expression levels of Bax, Bcl-2 and P53 genes by qRT-PCR in H596-TxR cells following combined overexpression of miR-17 and miR-16 and subsequent treatment with 12 nM paclitaxel. We observed that combined overexpression of miR-16 and miR-17 and subsequent paclitaxel treatment (12 nM) resulted in significant upregulation of Bax and P53 mRNA expressions with a concomitant downregulation of Bcl-2 (Fig. S5A–C).

We also evaluated the relative caspase-3 activity in these doubly transfected cells following paclitaxel treatment by caspase-3 assay kit. From caspase-3 assay we found that the relative caspase-3 activity increased significantly in the cells overexpressing both miRNAs (T24-miR-comb and TxR-miR-comb) than the cells overexpressing individual miRNAs (T24-miR-17 and TxR-miR-17 or T24-miR-16 and Txr-miR-16) or the negative control RNA (T24-miR-NC and TxR-miR-NC) (Figs. 8C

and S6D). Moreover, before paclitaxel exposure when these miRNA transfected cells were pre-treated with 50 μM zVAD-fmk for 2 h and then subjected to caspase-3 assay after paclitaxel treatment, they showed inhibited caspase-3 activity (Figs. 8C and S6D), again confirming apoptosis induced by combined overexpression of miR-17 and miR-16 and subsequent treatment with paclitaxel was caspase-3 dependent.

3.11. Combined overexpression of miR-17 and miR-16 and subsequent paclitaxel treatment resulted in the inhibition of PI3K/Akt/mTOR pathway in paclitaxel resistant lung cancer cells

Many recent studies have reported that the activation of PI3K/Akt signaling cascade plays a critical role in initiation and progression of tumor in several human cancers including NSCLC [36–38]. It has also been reported that several anti-tumor drugs induce apoptosis by inhibiting PI3K/Akt/mTOR dependent cell survival pathways [39]. So to assess whether this pathway was affected by combined overexpression of miR-16 and miR-17 in paclitaxel resistant A549-T24 cells, T24-miR-NC, T24-miR-17, T24-miR-16 and T24-miR-comb cells were treated with 12 nM paclitaxel for 48 h and protein levels of total and phosphorylated p85 (PI3K regulatory subunit) were analyzed after immuno-precipitating the cell lysates with an antibody against the p85 subunit of PI3K (Fig. 8D and E). We also evaluated the total and phosphorylated Akt levels in these cell lysates. We observed that T24-

miR-comb cells exhibited much lower levels of total and phosphorylated p85 and phosphorylated Akt with upregulated mTOR expression compared to T24-miR-17 or T24-miR-16 cells (Fig. 8D) indicating that combined overexpression of miR-17 and miR-16 followed by paclitaxel treatment resulted in inhibition of PI3K/Akt/mTOR signaling pathway at a greater extent, which in turn might contribute to the increased apoptosis and heightened cell death, observed in the case of these doubly transfected cells (T24-miR-comb).

3.12. Combined overexpression of miR-16 and miR-17 and subsequent paclitaxel treatment induced disruption of mitochondrial membrane potential and release of cytochrome-c from the mitochondria to cytosol in A549-T24 cells

Previous studies have reported that the activation of caspases is driven by the collapse of mitochondrial membrane potential, $\Delta\Psi$, as a result of depolarization and leakiness of the inner mitochondrial membrane and release of cytochrome-c from mitochondrial membrane to cytosol through intrinsic mitochondrial apoptotic pathway [1,40,41]. Therefore, we were interested to investigate the impact of combined overexpression of miR-17 and miR-16 and subsequent paclitaxel treatment (12 nM) on the mitochondrial membrane potential of A549-T24 cells using JC-1 dye. As shown in Fig. 9A and B, combined inhibition of Beclin-1 mediated autophagy by miR-17 overexpression and inhibition of Bcl-2 by miR-16 overexpression and subsequent paclitaxel treatment of A549-T24 cells resulted in collapse of $\Delta\Psi$ at much greater extent compared to T24-miR-17 or T24-miR-16 cells as observed by lower in red fluorescence intensity (JC-1). Thereafter, we checked the status of cytosolic cytochrome-c which gets released in the cytosol from the mitochondria following disruption of mitochondrial membrane potential. As shown in Fig. 9C, when A549-T24 cells were co-transfected with miR-17 and miR-16 and subsequently treated with 12 nM paclitaxel for 48 h, the amount of cytochrome-c released in the cytosol was much higher than that of T24-miR-17 and T24-miR-16 cells justifying increased mitochondrial damage and subsequent apoptosis.

3.13. Overexpression of miR-16 and miR-17 and subsequent paclitaxel treatment stimulated ROS generation in paclitaxel resistant lung cancer cells

Several recent studies have indicated the involvement of reactive oxygen species (ROS) in the induction of autophagy and apoptosis and demonstrated that ROS plays an important role in the release of cytochrome-c from the mitochondria [7,18,32,42,43]. In our previous study, we showed that inhibition of cyto-protective autophagy by miR-17 overexpression and subsequent Beclin-1 downregulation resulted in increased ROS generation upon paclitaxel treatment [1]. Moreover, recently several reports have provided evidence that inhibition of anti-apoptotic protein Bcl-2 results in increase in oxidative stress due to greater production of ROS in cancer cells following treatment with chemotherapeutic agents [44–47]. Therefore, we decided to analyze whether inhibition of Beclin-1 mediated autophagy by miR-17 overexpression and induction of apoptosis by Bcl-2 inhibition through miR-16 overexpression jointly could stimulate higher generation of ROS following paclitaxel treatment. We found consistent with our previous report, inhibition of cyto-protective autophagy miR-17 overexpression and subsequent paclitaxel treatment resulted in accumulation of ROS in T24-miR-17 cells than T24-miR-NC cells (Fig. 9D and E). Moreover, ROS generation was somewhat more pronounced in T24-miR-16 cells compared to T24-miR-17 and T24-miR-NC cells (Fig. 9D and E). When A549-T24 cells were co-transfected with both miR-17 and miR-16, significant increase in ROS level was observed (Fig. 9D and E), indicating combined overexpression of miR-17 and miR-16 followed by paclitaxel treatment stimulated ROS formation in greater extent. We also noticed similar increased accumulation of ROS following combined overexpression of miR-17 and miR-16 and paclitaxel treatment in H596-TxR cells (Fig. S7A and B).

Since the level of ROS was significantly elevated in T24-miR-comb and TxR-miR-comb cells, we were further interested to analyze whether attenuation of ROS could influence paclitaxel mediated apoptotic cell death. For this purpose, we pre-treated T24-miR-NC and TxR-miR-NC, T24-miR-17 and TxR-miR-17, T24-miR-16 and TxR-miR-16 and T24-miR-comb and TxR-miR-comb cells with 1 mM N-acetyl-L-cysteine (NAC) for 4 h, then exposed them to 12 nM paclitaxel for 48 h after changing the NAC containing media and cell viability was measured by MTT assay. As shown in Fig. 10I, pre-treatment with NAC inhibited the cytotoxic effects of paclitaxel by scavenging ROS. Similar results were observed with TxR-miR-comb cells (Fig. S8I) where pre-treatment with 1 mM NAC and subsequent paclitaxel treatment resulted in the marked increase in cell viability as measured by MTT assay. Moreover, to confirm whether this reduction in cell death was due to true reduction in cellular apoptosis or not, these treated cells were subjected to two color flow cytometric assay after staining with annexin V/PI. We observed that when these miRNA transfected cells were pre-treated with the 1 mM NAC for 4 h and then exposed to 12 nM paclitaxel for 48 h, the percentage of cells undergoing apoptosis reduced significantly irrespective of the cell type (Fig. 10A–D compared to Fig. 10E–H and Fig. S8A–D compared to Fig. S8E–H) suggesting that generation of ROS following combined overexpression of miR-17 and miR-16 and subsequent paclitaxel treatment played a critical role in regulating cell death response in paclitaxel resistant lung cancer cells.

4. Discussion

Paclitaxel based combination chemotherapy is widely used to treat and extend survival in patients diagnosed with lung cancer [5]. Although the exact mechanism of cytotoxicity of paclitaxel to cancer cells is not completely understood. The major mechanism underlying its anti-tumor activity has been ascribed to be binding of paclitaxel to the β-subunit of α–β tubulin heterodimer of microtubule, thereby interfering with the microtubular dynamicity, resulting in G_2/M mitotic arrest. Despite its ability to stabilize microtubule and impair mitosis, paclitaxel also induces apoptosis by directly interacting with the mitochondrial membrane proteins [48,49] and regulates cytokine gene expression suggesting multiple effect of paclitaxel in human cancer [50,51]. However, the clinical effectiveness of paclitaxel in the treatment of NSCLC is often negated by the emergence of paclitaxel resistance which appears following couple cycles of paclitaxel based chemotherapy. Although the exact mechanisms responsible for the development of paclitaxel resistance still remained elusive, upregulation of P-glycoprotein and related drug efflux pumps [52,53] and altered expression of tubulin isotypes, particularly βIII-tubulin [54,55] have been strongly implicated in paclitaxel resistance.

Dysregulation of miRNA expression has been shown to play an important role in the development of clinical resistance to paclitaxel. In recent years increasing studies have indicated that many miRNAs, having oncogenic or tumor suppressive function, have been identified to be involved in cell proliferation, apoptosis and drug resistance [1,3,20,56,57]. However, the exact mechanisms contributing to miRNA dysregulation leading to paclitaxel resistance remained poorly understood. We previously performed differential miRNA array analysis for screening differentially expressed miRNAs between paclitaxel sensitive and paclitaxel resistance lung cancer cells [1]. In that study we showed that paclitaxel resistant lung cancer cells exhibit reduced expression of miR-17 and this downregulation of miR-17 expression resulted in the upregulation of Beclin-1 and subsequent cytoprotective autophagy which protects the lung cancer cells against paclitaxel induce cytotoxicity and this in-turn helps the cells to develop paclitaxel resistance [1]. In this report, we showed that paclitaxel resistant lung cancer cells exhibited decreased expression of miR-16 (Fig. 1A). We performed qRT-PCR analysis using TaqMan miRNA assays and confirmed that miR-16 was

significantly downregulated in A549-T24 cells (Fig. 1A). To get a more generalized view and to extend our finding we also evaluated the relative miR-16 expression levels in three other in vitro generated paclitaxel resistant cell lines and found similar results (Fig. 1A). We also evaluated the relative expression level of miR-17 in these paclitaxel resistant cell lines and found similar downregulation of miR-17 expression compared to their respective paclitaxel sensitive counterparts (Fig. S1A). All these data collectively confirmed that downregulation of miR-16 and miR-17 following paclitaxel resistance was a general phenomenon and it is not limited to any particular cell line. Since, it has been previously reported that cellular expression of Bcl-2 is inversely modulated by miR-16 expression [21,22,56] we performed luciferase reporter assay to demonstrate that anti-apoptotic protein Bcl-2 was a direct target of miR-16 (Fig. 2).

In the previous decade inhibition of apoptosis induction by paclitaxel has been the major consideration in the development of cancer drug resistance [8]. Recently, stimulation of autophagy in response to paclitaxel treatment has also been implicated to contribute to the development of paclitaxel resistance in many types of cancer including NSCLC [1,7]. We have previously shown that paclitaxel resistant lung cancer cells exhibit heightened level of cellular autophagy with increased expression of Beclin-1 which plays a critical role in initiating and mediating cytoprotective autophagy [1]. Moreover, it has been previously reported that Bcl-2 and other anti-apoptotic proteins are overexpressed in several cancers and are associated with the development of chemoresistance and radioresistance [58–60]. We also observed upregulation of Bcl-2 in paclitaxel resistant lung cancer cells compared to paclitaxel sensitive parental cells (Figs. 3A and B and S2A and S2B). However, this appeared to be in conflict with reports showing that Bcl-2 inhibits autophagy by binding with Beclin-1 in cancer cells [24, 25]. It has also been shown that Bcl-2 binds to Beclin-1 and inhibits autophagy under nutrient rich conditions but gets dissociated from Beclin-1 following nutrient starvation and stressed condition [24]. Because of these reports, we thought perhaps that dissociation of Bcl-2 from Beclin-1 occurs in paclitaxel resistant A549 cells in the presence of paclitaxel stress. However, in a co-immunoprecipitation experiment we did not find any co-immunoprecipitated Beclin-1 with Bcl-2, although we successfully detected co-immunoprecipitated inositol 1,4,5-triphosphate receptor (IP3R) with Bcl-2 (Figs. 3C and S2C) in both A549-T24 and H596-TxR cells, while under similar condition Beclin-1 was found to be associated with Bcl-2 in parental A549 and H596 cells (Figs. 3C and S2C). Our observations collectively demonstrated that in paclitaxel resistant lung cancer cells, in the presence of paclitaxel, overexpression of Bcl-2 caused inhibition of apoptosis, which inturn facilitated the cells to undergo autophagy with increased expression of Beclin-1. Moreover, our data were consistent with the recent observation that Bcl-2 facilitates autophagy to occur by inhibiting apoptosis when cells are subjected to metabolic stress in the presence of DNA damaging agent etoposide or kinase inhibitor staurosporine [30,31].

Overexpression of Bcl-2 and other anti-apoptotic proteins has been shown to be associated with the development of chemoresistance [58,59]. In this report, we showed that overexpression of Bcl-2 was associated with downregulation of miR-16 expression in paclitaxel resistant lung cancer cells. Moreover, it has also been demonstrated that upregulation of Beclin-1 mediated autophagy following miR-17 downregulation played an important role in the development of paclitaxel resistance in lung cancer cells [1]. All these data indicated that simultaneous downregulation of miR-17 and miR-16 was involved in the development of paclitaxel in lung cancer cells upregulating relative expression of Beclin-1 and Bcl-2 respectively. This intrigued us to investigate the effect of combined overexpression of miR-16 and miR-17 in paclitaxel resistant lung cancer cells. We found that joint overexpression of both miR-16 and miR-17 significantly sensitized the paclitaxel resistant lung cancer cells to a lower dose of paclitaxel compared to cells overexpressed with either miR-17 or miR-16 individually (Figs.

4A and S3A). We also found that when A549-T24 cells were simultaneously overexpressed with both miR-16 and miR-17 and treated with paclitaxel they showed significantly reduced tumor forming ability suggesting that simultaneous downregulation of miR-16 and miR-17 plays a critical role in the development of paclitaxel resistance in lung cancer (Fig. 4C and D). Moreover, when paclitaxel sensitive parental lung cancer cells were co-overexpressed with both anti-miR-17 and anti-miR-16, they showed reduced sensitivity to paclitaxel clearly demonstrating direct association of miR-17 and miR-16 with paclitaxel resistance (Figs. 4B and S3B). We also identified higher percentage of apoptosis in cells co-transfected with miR-17 and miR-16 together after treatment with paclitaxel (Figs. 7 and S5) which was further confirmed by immunoblotting of the apoptotic marker proteins, cleaved PARP and through detection of caspase 3 activity (Figs. 8A–C and S6). These results suggested that induction of cytoprotective autophagy by paclitaxel treatment and inhibition of apoptosis by up-regulation of anti-apoptotic protein Bcl-2 jointly played key roles in the development of paclitaxel resistance in lung cancer cells. Furthermore, the PI3K/Akt/mTOR pathway plays a central role in maintaining aggressive malignant tumor growth and its activation mediates chemoresistance by promoting cell survival and inhibition of induction of apoptosis [61]. Here we showed that combined overexpression of miR-17 and miR-16 and subsequent paclitaxel treatment resulted in the greater inhibition of cell survival signaling via PI3K/Akt/mTOR pathway (Fig. 8D and E) and also transduced the downstream mitochondrial apoptotic signals important for initiation of apoptosis in paclitaxel resistant lung cancer cells [62].

Next, we wanted to know that by which mechanism inhibition of Beclin-1 expression by miR-17 overexpression and downregulation of Bcl-2 through miR-16 overexpression induced increased apoptosis in paclitaxel resistant lung cancer cells? We found significant drop in mitochondrial membrane potential following combined overexpression of miR-17 and miR-16 and subsequent paclitaxel treatment in A549-T24 cells (Fig. 9A and B). These dysfunctional mitochondria stimulated ROS generation in T24-miR-comb at a greater extent than T24-miR-17 and T24-miR-16 (Figs. 9D, E and S7). Moreover, scavenging of this ROS accumulation by anti-oxidant NAC pre-treatment following co-overexpression of miR-17 and miR-16 prevented paclitaxel induced apoptosis in lung cancer cells (Figs. 10 and S7). Our results indicated inhibition of mitochondrial membrane potential following combined overexpression of miR-17 and miR-16 and subsequent paclitaxel treatment resulted in the greater accumulation of ROS, which played a critical role in regulating cell death response in paclitaxel resistant lung cancer cells.

5. Conclusion

Our study showed that exposure of the cancer cells to paclitaxel triggered multiple pro-survival pathways. It resulted in the induction of autophagy by upregulating Beclin-1 and also resulted in inhibition of apoptosis by overexpressing Bcl-2 in paclitaxel resistant lung cancer cells. We also demonstrated that this upregulation of Beclin-1 and Bcl-2 was inversely correlated to the relative expression of miR-17 and miR-16 respectively which played important roles in the development of paclitaxel resistance in lung cancer cells. Moreover, when paclitaxel resistant lung cancer cells were jointly overexpressed with miR-17 and miR-16 and subsequently treated with paclitaxel, they showed significantly increased paclitaxel sensitivity suggesting that simultaneous induction of autophagy by Beclin-1 upregulation and inhibition of apoptosis by elevated expression of Bcl-2 were responsible for the development of paclitaxel resistance in lung cancer cells. Moreover, the role of combined overexpression of miR-17 and miR-16, we proposed here, offered the intriguing possibility that paclitaxel resistance could be reversed by inhibiting miR-17 and miR-16 downregulation and/or its downstream pathways. Furthermore, our results showed that the paclitaxel mediated cell death response following combined overexpression

of miR-16 and miR-17 was largely dependent on ROS generation suggesting that regulation of ROS accumulation following miR-16 and miR-17 overexpression could be a potential strategy to overcome paclitaxel resistance in lung cancer and merit further study.

Acknowledgments

Appendix A. Supplementary data

Supplementary data to this article can be found online at http://dx.doi.org/10.1016/j.cellsig.2014.11.023.

References

[1] A. Chatterjee, D. Chattopadhyay, G. Chakrabarti, PLoS One 9 (2014) e95716.
[2] J.S.H. Ferlay, F. Bray, D. Forman, C. Mathers, D.M. Parkin, Int. J. Cancer 127 (2010) 2893–2917.
[3] A. Holleman, I. Chung, R.R. Olsen, B. Kwak, A. Mizokami, N. Saijo, A. Parissenti, Z. Duan, E.E. Voest, B.R. Zetter, Oncogene 30 (2011) 4386–4398.
[4] D. Henley, M. Isbill, R. Fernando, J.S. Foster, J. Wimalasena, Cancer Chemother. Pharmacol. 59 (2007) 235–249.
[5] E.K. Rowinsky, R.C. Donehower, N. Engl. J. Med. 332 (1995) 1004–1014.
[6] L.P. Chen, S.M. Cai, J.X. Fan, Z.T. Li, Gynecol. Oncol. 56 (1995) 231–234.
[7] G. Xi, X. Hu, B. Wu, H. Jiang, C.Y. Young, Y. Pang, H. Yuan, Cancer Lett. 307 (2011) 141–148.
[8] G.M. Ajabnoor, T. Crook, H.M. Coley, Cell Death Dis. 3 (2012) e260.
[9] E.Y. Chi, B. Viriyapak, H.S. Kwack, Y.K. Lee, S.I. Kim, K.H. Lee, T.C. Park, Obstet. Gynecol. Sci. 56 (2013) 84.
[10] D.P. Bartel, Cell 116 (2004) 281–297.
[11] D.P. Bartel, Cell 136 (2009) 215–233.
[12] P.E. Blower, J.S. Verducci, S. Lin, J. Zhou, J.H. Chung, Z. Dai, C.G. Liu, W. Reinhold, P.L. Lorenzi, E.P. Kaldjian, C.M. Croce, J.N. Weinstein, W. Sadee, Mol. Cancer Ther. 6 (2007) 1483–1491.
[13] C. Mayr, M.T. Hemann, D.P. Bartel, Science 315 (2007) 1576–1579.
[14] K.J. Livak, T.D. Schmittgen, Methods 25 (2001) 402–408.
[15] W. Strober, Current Protocols in Immunology/Edited by John E. Coligan… [et al], 2001. (Appendix 3:Appendix 3B).
[16] Z. Xie, P.F. Choong, L.F. Poon, J. Zhou, J. Khng, V.J. Jasinghe, S. Palaniyandi, C.S. Chen, Cancer Chemother. Pharmacol. 62 (2008) 949–957.
[17] M.M. Bradford, Anal. Biochem. 72 (1976) 248–254.
[18] X. Pan, X. Zhang, H. Sun, J. Zhang, M. Yan, H. Zhang, PLoS One 8 (2013) e56679.
[19] E. Eruslanov, S. Kusmartsev, Methods Mol. Biol. 594 (2010) 57–72.
[20] A. Cimmino, G.A. Calin, M. Fabbri, M.V. Iorio, M. Ferracin, M. Shimizu, S.E. Wojcik, R.I. Aqeilan, S. Zupo, M. Dono, L. Rassenti, H. Alder, S. Volinia, C.G. Liu, T.J. Kipps, M. Negrini, C.M. Croce, Proc. Natl. Acad. Sci. U. S. A. 102 (2005) 13944–13949.
[21] M.G. Diniz, C.C. Gomes, W.H. de Castro, A.L. Guimaraes, A.M. De Paula, H. Amm, C. Ren, M. MacDougall, R.S. Gomez, Cell. Oncol. 35 (2012) 285–291.
[22] L. Xia, D. Zhang, R. Du, Y. Pan, L. Zhao, S. Sun, L. Hong, J. Liu, D. Fan, J. Int. Cancer 123 (2008) 372–379.
[23] T.Q. Yang, X.J. Lu, T.F. Wu, D.D. Ding, Z.H. Zhao, G.L. Chen, X.S. Xie, B. Li, Y.X. Wei, L.C. Guo, Y. Zhang, Y.L. Huang, Y.X. Zhou, Z.W. Du, Cancer Sci. 105 (2014) 265–271.
[24] S. Pattingre, A. Tassa, X. Qu, R. Garuti, X.H. Liang, N. Mizushima, M. Packer, M.D. Schneider, B. Levine, Cell 122 (2005) 927–939.
[25] S. Luo, D.C. Rubinsztein, Cell Death Differ. 17 (2010) 268–277.
[26] L. Xu, D. Kong, L. Zhu, W. Zhu, D.W. Andrews, T.H. Kuo, Mol. Cell. Biochem. 295 (2007) 153–165.
[27] S.A. Oakes, L. Scorrano, J.T. Opferman, M.C. Bassik, M. Nishino, T. Pozzan, S.J. Korsmeyer, Proc. Natl. Acad. Sci. U. S. A. 102 (2005) 105–110.
[28] R. Chen, I. Valencia, F. Zhong, K.S. McColl, H.L. Roderick, M.D. Bootman, M.J. Berridge, S.J. Conway, A.B. Holmes, G.A. Mignery, P. Velez, C.W. Distelhorst, J. Cell Biol. 166 (2004) 193–203.
[29] L.Y. Xue, S.M. Chiu, K. Azizuddin, S. Joseph, N.L. Oleinick, Photochem. Photobiol. 83 (2007) 1016–1023.
[30] K. Degenhardt, R. Mathew, B. Beaudoin, K. Bray, D. Anderson, G. Chen, C. Mukherjee, Y. Shi, C. Gelinas, Y. Fan, D.A. Nelson, S. Jin, E. White, Cancer Cell 10 (2006) 51–64.
[31] S. Shimizu, T. Kanaseki, N. Mizushima, T. Mizuta, S. Arakawa-Kobayashi, C.B. Thompson, Y. Tsujimoto, Nat. Cell Biol. 6 (2004) 1221–1228.
[32] R. Ofir, R. Seidman, T. Rabinski, M. Krup, V. Yavelsky, Y. Weinstein, M. Wolfson, Cell Death Differ. 9 (2002) 636–642.
[33] J. Li, N. Hou, A. Faried, S. Tsutsumi, H. Kuwano, Eur. J. Cancer 46 (2010) 1900–1909.
[34] D. Liu, Y. Yang, Q. Liu, J. Wang, Med. Oncol. 28 (2011) 105–111.
[35] Q. Zhang, S. Si, S. Schoen, J. Chen, X.B. Jin, G. Wu, J Exp Clin Cancer Res. 32 (2013) 1–11.
[36] C.X. Xu, H. Jin, J.Y. Shin, J.E. Kim, M.H. Cho, Front. Biosci. 2 (2010) 1472–1484.
[37] B.T. Hennessy, D.L. Smith, P.T. Ram, Y. Lu, G.B. Mills, Drug Discov. 4 (2005) 988–1004.
[38] I. Vivanco, C.L. Sawyers, Cancer 2 (2002) 489–501.
[39] L. Paz-Ares, C. Blanco-Aparicio, R. Garcia-Carbonero, A. Carnero, Clin. Transl. Oncol. 11 (2009) 572–579.
[40] H.I. Lin, Y.J. Lee, B.F. Chen, M.C. Tsai, J.L. Lu, C.J. Chou, G.M. Jow, Cancer Lett. 230 (2005) 248–259.
[41] M.A. Gallego, B. Joseph, T.H. Hemstrom, S. Tamiji, L. Mortier, G. Kroemer, P. Formstecher, B. Zhivotovsky, P. Marchetti, Oncogene 23 (2004) 6282–6291.
[42] D.B. Munafo, M.I. Colombo, J. Cell Sci. 114 (2001) 3619–3629.
[43] G. Varbiro, B. Veres, F. Gallyas Jr., B. Sumegi, Free Radic. Biol. Med. 31 (2001) 548–558.
[44] E.D. Lagadinou, A. Sach, K. Callahan, R.M. Rossi, S.J. Neering, M. Minhajuddin, J.M. Ashton, S. Pei, V. Grose, K.M. O'Dwyer, J.L. Liesveld, P.S. Brookes, M.W. Becker, C.T. Jordan, Cell Stem Cell 12 (2013) 329–341.
[45] P. Agostinis, Blood 102 (2003) 3079.
[46] L. Wang, P. Chanvorachote, D. Toledo, C. Stehlik, R.R. Mercer, V. Castranova, Y. Rojanasakul, Mol. Pharmacol. 73 (2008) 119–127.
[47] D.A. Hildeman, T. Mitchell, B. Aronow, S. Wojciechowski, J. Kappler, P. Marrack, Proc. Natl. Acad. Sci. U. S. A. 100 (2003) 15035–15040.
[48] C. Ferlini, L. Cicchillitti, G. Raspaglio, S. Bartollino, S. Cimitan, C. Bertucci, S. Mozzetti, D. Gallo, M. Persico, C. Fattorusso, G. Campiani, G. Scambia, Cancer Res. 69 (2009) 6906–6914.
[49] S. Haldar, J. Chintapalli, C.M. Croce, Cancer Res. 56 (1996) 1253–1255.
[50] M. Foss, B.W. Wilcox, G.B. Alsop, D. Zhang, PLoS One 3 (2008) e1476.
[51] S.B. Horwitz, Trends Pharmacol. Sci. 13 (1992) 134–136.
[52] L.M. Greenberger, L. Lothstein, S.S. Williams, S.B. Horwitz, Proc. Natl. Acad. Sci. U. S. A. 85 (1988) 3762–3766.
[53] T. Oguri, H. Ozasa, T. Uemura, Y. Bessho, K. Miyazaki, K. Maeno, H. Maeda, S. Sato, R. Ueda, Mol. Cancer Ther. 7 (2008) 1150–1155.
[54] C. Dumontet, S. Isaac, P.J. Souquet, F. Bejui-Thivolet, Y. Pacheco, N. Peloux, A. Frankfurter, R. Luduena, M. Perol, Bull. Cancer 92 (2005) E25–E30.
[55] S. Mozzetti, C. Ferlini, P. Concolino, F. Filippetti, G. Raspaglio, S. Prislei, D. Gallo, E. Martinelli, F.O. Ranelletti, G. Ferrandina, G. Scambia, Clin. Cancer Res. 11 (2005) 298–305.
[56] D. Bonci, V. Coppola, M. Musumeci, A. Addario, R. Giuffrida, L. Memeo, L. D'Urso, A. Pagliuca, M. Biffoni, C. Labbaye, M. Bartucci, G. Muto, C. Peschle, R. De Maria, Nat. Med. 14 (2008) 1271–1277.
[57] Y. Fujita, K. Kojima, R. Ohhashi, N. Hamada, Y. Nozawa, A. Kitamoto, A. Sato, S. Kondo, T. Kojima, T. Deguchi, M. Ito, J. Biol. Chem. 285 (2010) 19076–19084.
[58] M. Emi, R. Kim, K. Tanabe, Y. Uchida, T. Toge, Breast Cancer Res. 7 (2005) R940–R952.
[59] B.N. Fahy, M.G. Schlieman, M.M. Mortenson, S. Virudachalam, R.J. Bold, Cancer Chemother. Pharmacol. 56 (2005) 46–54.
[60] Y. Gazitt, M.L. Rothenberg, S.G. Hilsenbeck, V. Fey, C. Thomas, W. Montegomrey, Int. J. Oncol. 13 (1998) 839–848.
[61] G. Xu, W. Zhang, P. Bertram, X.F. Zheng, H. McLeod, Int. J. Oncol. 24 (2004) 893–900.
[62] Y. Fujiwara, Y. Hosokawa, K. Watanabe, S. Tanimura, K. Ozaki, M. Kohno, Mol. Cancer Ther. 6 (2007) 1133–1142.